Proteasome Activation by Small Molecules

Leestemaker, Y.; Jong, A. de; Witting, K.F.; Penning, R.; Schuurman, K.; Rodenko, B.; ... ; Ovaa, H.

Article

Cell Chemical Biology

Proteasome Activation by Small Molecules

Highlights

- Identification of more than ten small-molecule proteasome activators
- Proteasome activators increase degradation of model substrates
- P38 MAPK inhibition increases the clearance of toxic α-synuclein aggregates

Authors

Yves Leestemaker, Annemieke de Jong, Katharina F. Witting, ..., Wiep Scheper, Celia R. Berkers, Huib Ovaa

Correspondence

c.r.berkers@uu.nl (C.R.B.), h.ovaa@lumc.nl (H.O.)

In Brief

Small-molecule drugs that increase 26S proteasome have many potential therapeutic applications, including in neurodegenerative diseases. Here, Leestemaker et al. describe the identification of more than ten small-molecule compounds that increase proteasome activity and increase the clearance of model substrates.

Leestemaker et al., 2017, Cell Chemical Biology *24*, 725–736
June 22, 2017
http://dx.doi.org/10.1016/j.chembiol.2017.05.010

CellPress

Cell Chemical Biology
Article

Proteasome Activation by Small Molecules

Yves Leestemaker,[1,2,8] Annemieke de Jong,[1,8] Katharina F. Witting,[1,2] Renske Penning,[3] Karianne Schuurman,[1,9] Boris Rodenko,[1,10] Esther A. Zaal,[3] Bert van de Kooij,[4] Stefan Laufer,[5] Albert J.R. Heck,[3] Jannie Borst,[4] Wiep Scheper,[6,7] Celia R. Berkers,[3,*] and Huib Ovaa[1,2,11,*]

[1]Division of Cell Biology II, The Netherlands Cancer Institute, 1066 CX Amsterdam, the Netherlands
[2]Department of Chemical Immunology, Leiden University Medical Center, 2300 RC Leiden, the Netherlands
[3]Biomolecular Mass Spectrometry and Proteomics, Utrecht University, 3584 CH Utrecht, the Netherlands
[4]Division of Immunology, The Netherlands Cancer Institute, 2300 RC Amsterdam, the Netherlands
[5]Institute of Pharmacy, University of Tübingen, 72076 Tübingen, Germany
[6]Department of Clinical Genetics and Alzheimer Center, VU University Medical Center
[7]Department of Functional Genome Analysis, VU University
1081 HV Amsterdam, the Netherlands
[8]These authors contributed equally
[9]Present address: Division of Molecular Pathology, The Netherlands Cancer Institute, 2300 RC Amsterdam, the Netherlands
[10]Present address: UbiQ Bio BV, 1098 XH, Amsterdam, the Netherlands
[11]Lead Contact
*Correspondence: c.r.berkers@uu.nl (C.R.B.), h.ovaa@lumc.nl (H.O.)
http://dx.doi.org/10.1016/j.chembiol.2017.05.010

SUMMARY

Drugs that increase 26S proteasome activity have potential therapeutic applications in the treatment of neurodegenerative diseases. A chemical genetics screen of over 2,750 compounds using a proteasome activity probe as a readout in a high-throughput live-cell fluorescence-activated cell sorting-based assay revealed more than ten compounds that increase proteasome activity, with the p38 MAPK inhibitor PD169316 being one of the most potent ones. Genetic and chemical inhibition of either p38 MAPK, its upstream regulators, ASK1 and MKK6, and downstream target, MK2, enhance proteasome activity. Chemical activation of the 26S proteasome increases PROTAC-mediated and ubiquitin-dependent protein degradation and decreases the levels of both overexpressed and endogenous α-synuclein, without affecting the overall protein turnover. In addition, survival of cells overexpressing toxic α-synuclein assemblies is increased in the presence of p38 MAPK inhibitors. These findings highlight the potential of activation of 26S proteasome activity and that this can be achieved through multiple mechanisms by distinct molecules.

INTRODUCTION

The ubiquitin-proteasome system (UPS) is the main cellular machinery responsible for the degradation of intracellular proteins in eukaryotic cells and key to the regulation of cellular processes including proliferation, cell-cycle control, transcriptional regulation, and stress response (Glickman and Ciechanover, 2002). Upon modification with specific ubiquitin chains that function as a degradation signal, proteins are recognized and subsequently degraded by the 26S proteasome. The 26S proteasome is composed of a 20S catalytic core particle (CP) capped on one or both sides by a 19S regulatory particle (RP). The 20S CP consists of four stacked rings that contain seven subunits each and has an overall architecture of α(1–7)β(1–7)β(1–7)α(1–7). The two outer α rings provide binding sites for the 19S RPs and form a gated channel that controls access to the catalytic chamber. The catalytic activity resides within the two inner β rings and is provided by three constitutive subunits, termed β1, β2, and β5, that display caspase-like, tryptic-like, and chymotryptic-like activity, respectively. The 19S RP is responsible for the recognition and unfolding of protein substrates and, upon ATP binding, opens the gated channel of the 20S CP, allowing translocation of the substrates into the 20S CP (Glickman and Ciechanover, 2002). In lymphoid tissues, or after induction with the proinflammatory cytokines, interferon-γ or tumor necrosis factor alpha, the constitutive β subunits can be replaced by their immunoproteasome counterparts, termed β1i, β2i, and β5i, to form the immunoproteasome or mixed-type hybrid proteasomes (Dahlmann et al., 2000; Pelletier et al., 2010). In addition, two cell type-specific proteasome subtypes with differing subunit composition have been described, the thymoproteasome and the spermatoproteasome (Kniepert and Groettrup, 2014).

As the 26S proteasome is involved in many important regulatory processes, it is an attractive target for therapeutic intervention. The potential of proteasome-modulating drugs is illustrated by the success of the proteasome inhibitor bortezomib (Hideshima et al., 2001), which is used for the treatment of multiple myeloma and mantle cell lymphoma. Compounds that increase proteasome activity may also be of significant therapeutic value. Proteasome function becomes gradually impaired during aging and many age-related neurodegenerative disorders, including Parkinson's disease (PD), Alzheimer's disease (AD), and amyotrophic lateral sclerosis (ALS) are characterized by the presence of toxic intracellular protein aggregates that correlate with a reduction in proteasome activity (Kristiansen et al., 2007; Rubinsztein, 2006). In turn, oligomeric aggregates of proteins such as prion protein, tau, and α-synuclein have been shown

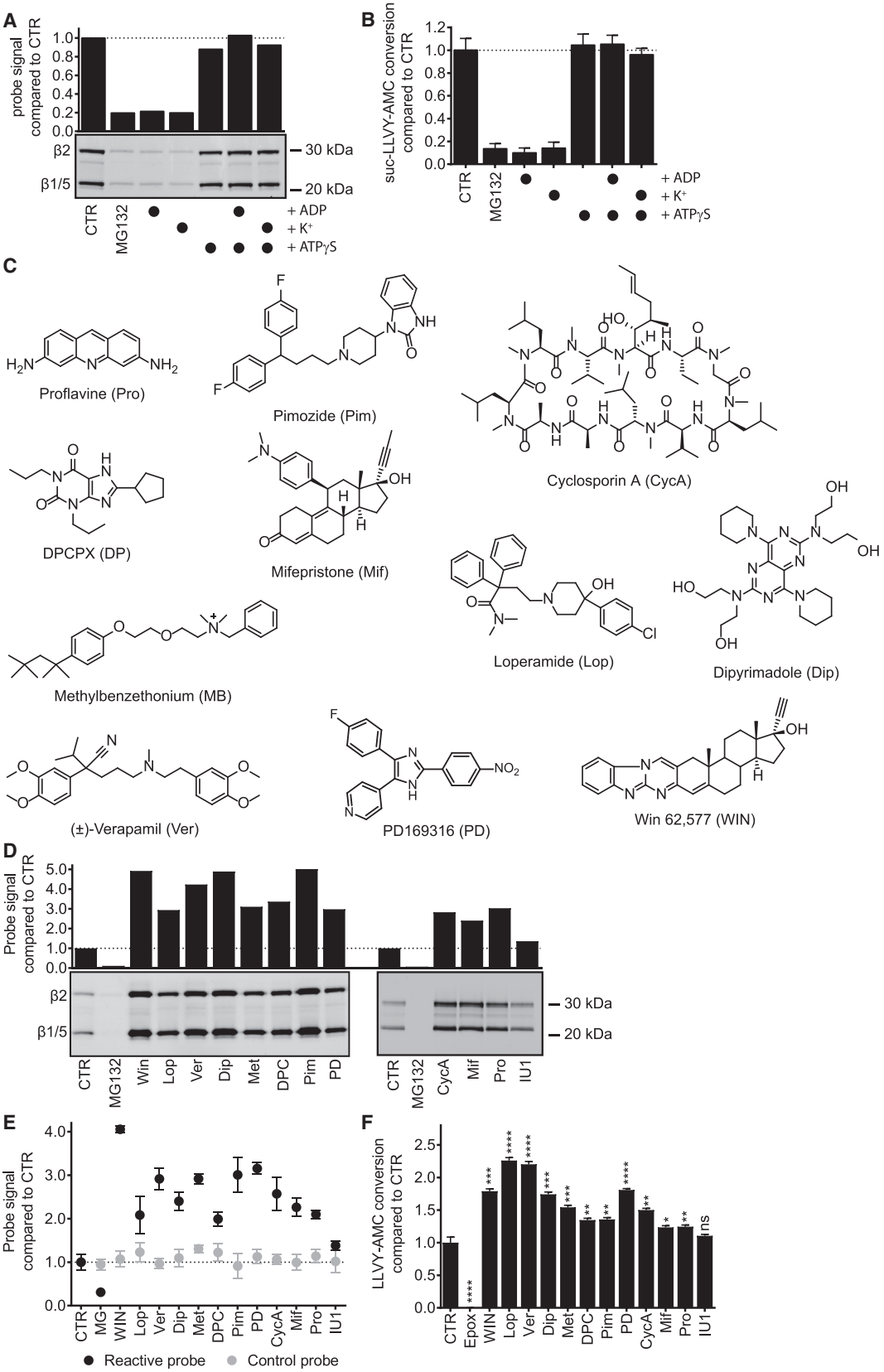

(legend on next page)

to bind to proteasomes in vitro and in vivo, thereby inhibiting its activity (Dantuma and Bott, 2014; Kristiansen et al., 2007; Myeku et al., 2016; Snyder et al., 2003). Moreover, inhibition of the proteasome results in the induction of α-synuclein aggregation, characteristic of PD, and neurodegeneration in a mouse model (Ebrahimi-Fakhari et al., 2011). This suggests a central role for the proteasome in a vicious cycle in neurodegenerative disease pathogenesis. Enhancing UPS activity, by either increasing the pool of free ubiquitin (Lee et al., 2009) or overexpressing specific ubiquitin ligases (Al-Ramahi et al., 2006; Tsai et al., 2003), can reduce toxicity induced by protein aggregates. Also enhancing proteasome activity by small-molecule compounds has been postulated to be of therapeutic value in the treatment of neurodegenerative diseases (Dantuma and Bott, 2014; Lee et al., 2010a). But, although a subset of proteasome activity-enhancing compounds has been reported, only very few have been shown to activate proteasomes in vivo. Sulforaphane increases proteasome levels in vivo through induction of the transcription factor Nrf2 (Liu et al., 2014). IU1 enhances proteasomal degradation by inhibiting USP14, a proteasome-associated deubiquitinating enzyme (Lee et al., 2010a). Rolipram enhances 26S proteasome activity and reduces levels of aggregated tau in vivo by activating protein kinase A (PKA) (Myeku et al., 2016).

The lack of suitable screening assays hinders the identification of small-molecule compounds that enhance proteasome activity. Current assays can only be used in vitro or monitor degradation by introducing tagged and often overexpressed model substrates. Such limitations can be overcome by the use of chemical probes, which allows for identification of novel proteasome activity-modulating compounds in primary cells, established cell lines, or in tissues. In this study we deploy such an activity-based probe (Berkers et al., 2007; de Jong et al., 2012) to identify new drug-like small molecules that can increase 26S proteasome activity in cells. Using this approach, we identify 11 novel compounds that enhance proteasome activity up to 4-fold in cells. In addition, we identify an important novel role for chemical and genetic inhibitors of p38α MAPK in activating the proteasome and enhancing degradation of specific proteins, including α-synuclein.

RESULTS

Identification of Novel Small-Molecule Proteasome Activators

To identify novel small molecules that are able to activate proteasome in intact cells, we used the cell-permeable fluorescent proteasome activity reporter Me_4BodipyFLAhx$_3$L$_3$VS (probe **1**; Figure S1A). Probe **1** covalently binds to catalytically active subunits of the proteasome in living cells in an activity-dependent manner. Hence, treatment of cells with negative or positive modulators of proteasome activity followed by probe treatment results in reduced or increased intracellular fluorescence, respectively, which can be measured by flow cytometry or SDS-PAGE followed by fluorescence scanning (Berkers et al., 2007; de Jong et al., 2012).

To further characterize probe **1**, we first performed time-dependent experiments by flow cytometry (Figure S1B) using both probe **1** and its inactive counterpart, in which the vinyl sulfone moiety is reduced by hydrogenation (reduced probe **1**; Figure S1A). Whereas the intracellular fluorescence using probe **1** increases linearly over time, the (background) fluorescence observed using the reduced probe stays constant over time, indicating that probe **1** can be used to assay the rate of reaction of the proteasome in cells. Next, we determined whether probe **1** accesses the proteasome via the gated channel, as protein substrates would, or whether it can diffuse into the proteasome without entering through the gate. To this end, the gated channel of the proteasome was chemically opened in MelJuSo (human melanoma) cell lysates by adding non-hydrolyzable ATP-γS (Li and Demartino, 2009) or closed by adding ADP and K^+ (Köhler et al., 2001; Peth et al., 2009) (Figure S1C). Subsequently, proteasome activity was profiled by separating subunits using SDS-PAGE. As can be seen in Figure 1A, ADP and K^+ treatment strongly reduced probe binding compared with untreated control, comparable with treatment with proteasome inhibitor MG132. Interestingly, ATP-γS did not increase proteasome activity, as assayed by probe **1** binding or by measuring the conversion of the fluorogenic proteasome substrate suc-LLVY-AMC (suc-LeuLeuValTyr-aminomethylcoumarin) (Figure 1B), indicating that in our hands the gated channel is already fully opened in MelJuSo cell lysates. As expected, opening or closing of the gated channel following probe addition did not change probe binding (Figure S1D). These data indicate that (like proteinaceous substrates) proteasome probes only enter the 20S particle if the gated channel is in an open conformation. Thus, although probe binding does not fully mimic the normal ubiquitin-mediated proteasomal protein degradation route, proteasome probes are suitable tools to screen for proteasome activation.

Next, we took a forward chemical genetics approach to identify proteasome-activating compounds and used probe **1** to screen both the Library of Pharmacologically Active Compounds and Johns Hopkins Clinical Compound Library in a

Figure 1. Identification of Small-Molecule Proteasome Activators Using a Proteasome Activity Probe

(A and D) In-gel fluorescence scan showing representative proteasome activity profiles in (A) MelJuSo cell lysates treated with MG132 or (combinations of) ADP, K^+, or ATP-γS or (D) MelJuSo cells after a 16 hr incubation with 5 μM compound or 750 nM MG132. Bars represent the quantified probe signal.

(B) Rate of suc-LLVY-AMC conversion in MelJuSo cell lysates treated with MG132 or (combinations of) ADP, K^+, or ATP-γ. Error bars represent SD of three independent experiments.

(C) Structures of small-molecule compounds that increase proteasome activity.

(E) Intracellular fluorescence intensities in MelJuSo cells after a 16 hr incubation with 5 μM of the indicated compounds, followed by incubation with either probe **1** or reduced probe **1** (termed reactive probe and control probe, respectively). All signals were normalized to intensities obtained in DMSO-treated control (CTR) cells. Error bars represent SD of three independent experiments.

(F) The rate of suc-LLVY-AMC conversion in MelJuSo cells treated with 5 μM of the indicated compounds. The conversion rates in DMSO-treated control (CTR) cells and epoxomicin-treated cells (Epox) were set to 1 and 0, respectively. Error bars represent SD of three independent experiments. Statistical significance: ns, not significant, *$p \leq 0.05$, **$p \leq 0.01$, ***$p \leq 0.001$, and ****$p \leq 0.0001$. See also Figures S1 and S2.

high-throughput flow cytometry-based assay (Figure S1E). Validation of the primary screening results by both flow cytometry and gel-based proteasome activity assays yielded 11 compounds that increased proteasome activity from 2- to 4-fold at concentrations of 5 μM (Figures 1C, 1D, and 1E), without any apparent toxicity as determined by a cell-titer blue cell viability assay (Figure S1F). In addition, we did not observe any changes in the overall levels of ubiquitinated proteins (Figure S1G). SDS-PAGE readouts of proteasome activity showed that all the identified compounds enhanced proteasome activity by increasing the activity of both the β1/5 and the β2 subunits (Figure 1D). Three other compounds activated the proteasome to a lesser extent (Figures S1H and S1I). The effects of all the compounds on proteasome activity could be confirmed in a panel of human cell lines, including HeLa, MCF-7, HEK293T, and THP-1 cells (Figure S2). When we tested the effect of IU1 under the same conditions, we observed little effect on the proteasome activity (Figures 1D, 1E, and S2A). However, when we used higher concentrations of IU1 (up to 25 μM), we did observe an increase in proteasome activity (Figures S2B and S2C). One of the compounds identified as a proteasome activator is Verapamil, a known inhibitor of drug efflux pump proteins, such as P-glycoprotein (Perrotton et al., 2007), suggesting that this could be a false-positive hit. In the original screen, however, Verapamil was present as a racemic mixture. When we tested the R- and S-enantiomers separately we observed that the R-enantiomer of Verapamil activated proteasome activity more strongly than the S-enantiomer (Figure S1J). Interestingly, S-Verapamil is a far more potent inhibitor of P-glycoprotein activity than R-Verapamil. To exclude the possibility that the observed increase in proteasome labeling induced by any of the other compounds was due to increased uptake or retention of the probe, we repeated the fluorescence-activated cell sorting assay with reduced probe **1**. Using this control probe, no increase in intracellular fluorescence was observed with any of the compounds, indicating that the cellular uptake and retention of probe **1** were unaffected by all compounds (Figure 1E). Furthermore, all compounds increased the intracellular degradation rate of suc-LLVY-AMC in an orthogonal proteasome activity assay up to 2.5-fold (Figure 1F). The overall levels of proteasome activation are lower when measured through suc-LLVY-AMC degradation compared with probe **1** binding. Likely, the high background levels that are measured when using fluorogenic substrates in cells make assays using probe **1** more sensitive than small fluorogenic substrate-based assays. Together, these data show that the observed increase in probe labeling can be attributed to an increase in proteasome activity, and verify that all 11 compounds are able to activate proteasomes and increase substrate turnover in intact cells.

Inhibition of p38α MAPK and Its Downstream Target MK2 Both Activate the Proteasome

One of the identified compounds, PD163916, is an established active-site inhibitor (type 1 inhibitor) of p38 MAPK. p38 MAPK-dependent phosphorylation has previously been shown to reduce proteasome activity in response to osmotic stress (Lee et al., 2010b). Moreover, the presence of activated p38 has been observed in neurodegenerative diseases, including ALS (Bendotti et al., 2004; Tortarolo et al., 2003) and AD (Atzori et al., 2001; Zhu et al., 2000). Hence, we next focused on p38 MAPK-inhibiting compounds. A panel of p38 MAPK inhibitors was tested for their ability to increase intracellular proteasome activity in MelJuSo cells, including SB202190 and SB203580 (both PD169316 analogs and fully ATP-competitive type 1 inhibitors) and the structurally different p38α inhibitor skepinone-L, which is highly selective due to induced glycine-flip at the hinge region of the kinase (Koeberle et al., 2012) (Figure 2A). As expected, all inhibitors activated the proteasome in a dose-dependent manner as assayed using the probe-based flow cytometry assay (Figure 2B). In addition, all p38 MAPK inhibitors increased the activity of both the β1/5 and β2 subunits, without affecting subunit abundance (Figure 2C), cell viability (Figure S3A), or the overall levels of ubiquitinated proteins (Figure S3B). All compounds were also able to increase the intracellular turnover of suc-LLVY-AMC (Figure 2D).

Four p38 MAPK isoforms have been described (α, β, γ, and δ), with p38α MAPK being the major isoform (Borst et al., 2013), which could be confirmed in MelJuSo cells by analyzing p38 mRNA levels (Figure S3C). To investigate which isoforms mediate the observed proteasome-activating effect, all p38 MAPK isoforms were individually depleted from MelJuSo cells using small interfering RNA (siRNA), followed by incubation with a proteasome activity probe. While siRNA depletion decreased the levels of all the individual isoforms by at least 80% (Figure S3D), only p38α knockdown resulted in a substantial increase in proteasome activity (Figure 2E). In contrast, knockdown of p38β only slightly enhanced proteasome activity, while no effect on proteasome activity was observed upon depletion of either p38γ or p38δ isoforms. These data are in line with the isoform preference of the used p38 inhibitors that are all slightly preferential for the α versus the β isoform, but do not inhibit the γ and δ isoforms (Koeberle et al., 2012). Gel-based activity assays confirmed that p38α depletion resulted in an enhanced activity of both β1/5 and β2 subunits, without affecting the protein levels of β subunits (Figure 2F). Treatment with PD169316 following the depletion of p38α from MelJuSo cells did not further increase proteasome activity (Figure 2G), confirming that the p38 MAPK inhibitors described here activate the intracellular proteasome pool by directly inhibiting p38 MAPK and not through an off-target effect.

Finally, we asked which up- and downstream players in the p38 MAPK pathway were involved in the p38α-dependent activation of the proteasome. To this end, we performed a siRNA screen in MelJuSo cells against kinases that have previously been implicated in the MAPK signaling pathways. Of these kinases, only knock down of the upstream p38 regulators ASK1 (apoptosis signal-regulating kinase 1) and MKK6 (MAP kinase kinase 6), as well as the p38 MAPK target protein MK2, resulted in an over 2-fold enhancement of intracellular proteasome activity as measured by flow cytometry (Figures 3A and S3E). Both gel-based activity assays and measurements of the intracellular suc-LLVY-AMC conversion confirmed that ASK1 and MK2 knockdown enhanced the intracellular proteasome activity, without changing the protein levels of β5 subunits (Figures 3B, 3C, and S3F). No significant increase in suc-LLVY-AMC conversion was observed for cells treated with siRNAs against MKK6 (Figure 3B), probably because this assay is less sensitive than probe-based assays.

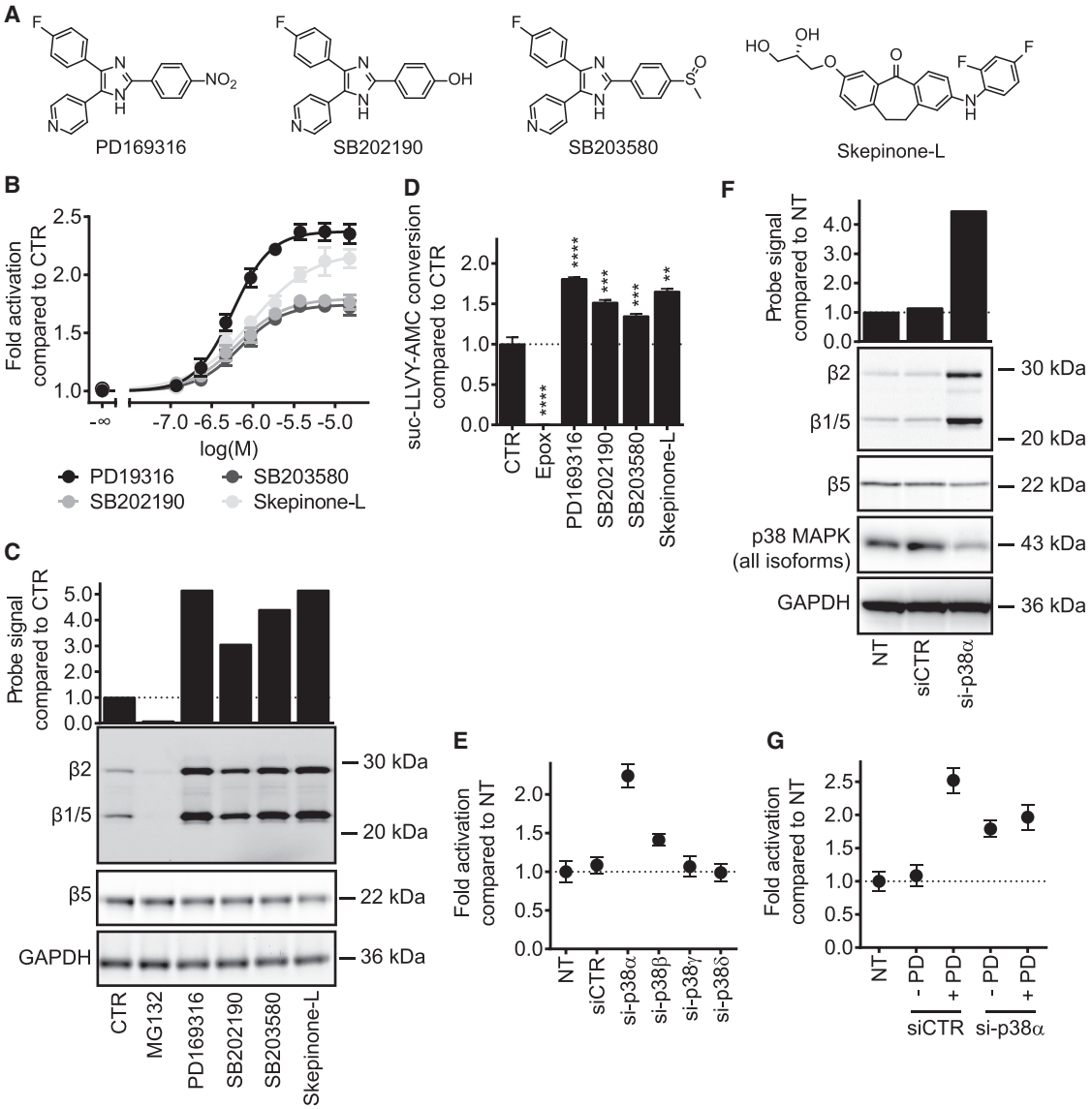

Figure 2. Chemical and Genetic Inhibition of p38 MAPK Increase Intracellular Proteasome Activity

(A) Structures of p38 MAPK active-site inhibitors PD169316, SB202190, SB203580, and p38 MAPK allosteric inhibitor skepinone-L.

(B) Intracellular fluorescence intensities in MelJuSo cells, treated with probe **1** after a 16 hr incubation period with increasing concentrations of the indicated p38 MAPK inhibitors. All signal intensities were normalized to intensities obtained in DMSO-treated control (CTR) cells. Error bars represent SD of three independent experiments.

(C) In-gel fluorescence scan (top) showing representative proteasome labeling profiles in MelJuSo cells after a 16 hr incubation period with 5 μM of the indicated compounds or 750 nM MG132. Bars represent the quantified probe signal. Immunoblot analysis of the levels of the indicated proteins (bottom). GADPH levels were used as a loading control.

(D) The rate of suc-LLVY-AMC conversion in MelJuSo cells treated with 5 μM of the indicated compounds. The conversion rates in DMSO-treated control (CTR) cells and epoxomicin-treated cells were set to 1 and 0, respectively. Error bars represent SD of three independent experiments. Statistical significance: ns, not significant, $^{**}p \leq 0.01$, $^{***}p \leq 0.001$, and $^{****}p \leq 0.0001$.

(E) Intracellular fluorescence intensities in MelJuSo cells, treated with probe **1** after 72 hr transfection with siRNAs targeting the indicated proteins or control siRNA (siCTR). All signal intensities were normalized to intensities obtained in non-transfected (NT) cells. Error bars represent SD of three independent experiments.

(F) In-gel fluorescence scan (top) showing representative proteasome labeling profiles in MelJuSo cells after 72 hr transfection with either control siRNA or siRNA targeting p38α MAPK. Bars represent the quantified probe signal. Immunoblot analysis of the levels of the indicated proteins (bottom). GADPH levels were used as a loading control.

(G) Intracellular fluorescence intensities in MelJuSo cells, treated with probe **1** after 72 hr transfection with siRNAs targeting the indicated proteins or control siRNA (siCTR), followed by a 16 hr incubation with PD169316 or DMSO. All signal intensities were normalized to intensities obtained in NT cells. Error bars represent SD of three independent experiments.

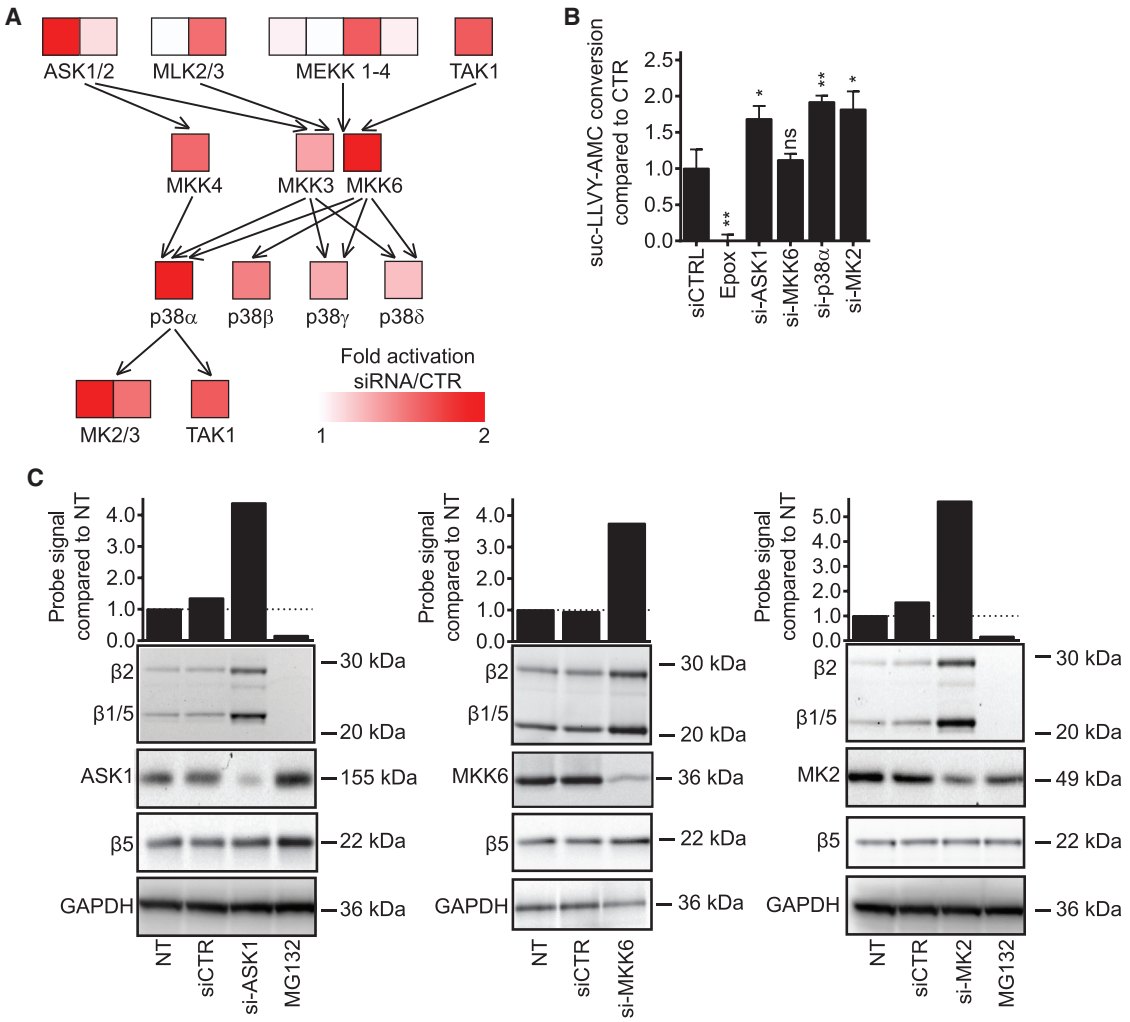

Figure 3. Involvement of p38 MAPK Pathway in Proteasome Modulation

(A) Normalized intracellular fluorescence intensities in probe **1**-treated MelJuSo cells after 72 hr transfection with siRNAs targeting the indicated proteins in the p38 MAPK pathway. The color of the box indicates fold activation of siRNA over control siRNA.

(B) Rate of suc-LLVY-AMC conversion in MelJuSo cells after 72 hr transfection with siRNA targeting the indicated proteins. The conversion rates in cells transfected with control siRNA (siCTR) and epoxomicin-treated cells were set to 1 and 0, respectively. Error bars represent SD of three independent experiments. Statistical significance: ns, not significant, *$p \leq 0.05$, and **$p \leq 0.01$.

(C) In-gel fluorescence scan (top) showing representative proteasome labeling profiles in MelJuSo cells after 72 hr transfection with either control siRNA or siRNA targeting the indicated proteins. Bars represent the quantified probe signal. Immunoblot analysis (bottom) showing the expression levels of the indicated proteins. GAPDH levels were used as a loading control. See also Figures S3 and S4, Tables S1 and S2.

p38 MAPK-Mediated Proteasome Activation and Inhibition Work through Distinct Mechanisms

To investigate whether p38 MAPK inhibitor-treated cells retain their increased activity also after cell lysis, HEK293 cells stably expressing HTBH (histidine tag-TEV cleavage sequence-biotin tag-histidine tag) tagged Rpn11 (Wang et al., 2007) (a 19S RP subunit) were treated with PD169316, skepinone-L, or MK2 inhibitor III (Anderson et al., 2007) (Figure 4A). Alternatively, p38α was depleted from these cells using siRNA. Subsequently, proteasomes from these cells were affinity purified (Figures S4A and S4B) as described previously (Wang et al., 2007), and the activity of these isolated proteasomes was measured. Both the probe-based proteasome activity assay and measurement of suc-LLVY-AMC hydrolysis showed that proteasomes, once activated in cells, retain their enhanced activity, even after mild cell lysis and purification (Figures 4B and 4C). This suggests that proteasome activation by p38 MAPK inhibition does occur through direct modulation of proteasome complexes, for example via post-translationally modification of these complexes.

Previous studies have shown that both overexpressed p38 MAPK and ASK1 phosphorylate the 19S RP, at Thr-273 of the Rpn2 subunit and on Rpt5, respectively (Lee et al., 2010b; Um et al., 2010), resulting in proteasome inhibition. Therefore, we next determined whether changes in the phosphorylation status of the proteasome could also be responsible for the observed activation by p38 MAPK inhibition. To this end, we analyzed changes in the phosphorylation status of cells treated with PD169316, skepinone-L, or MK2 inhibitor III using a proteomics

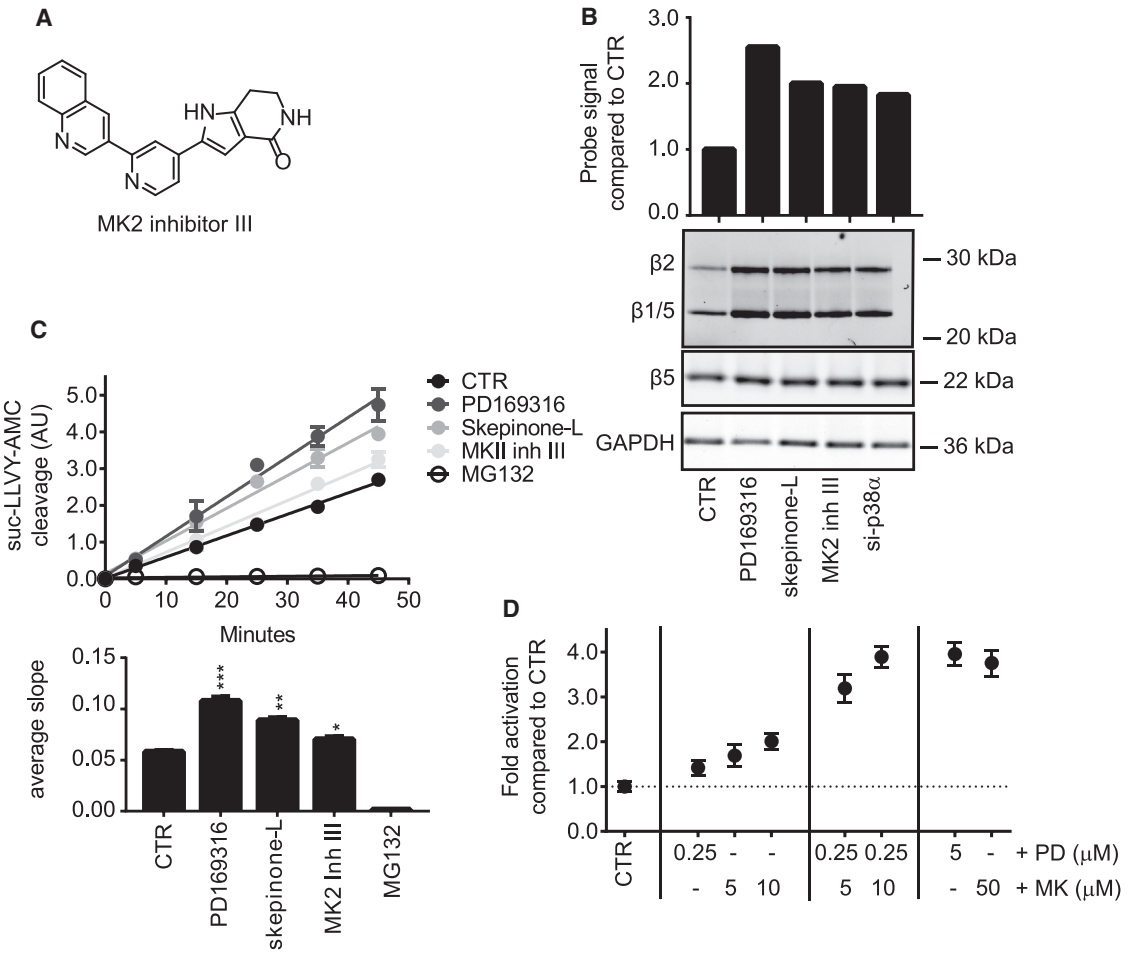

Figure 4. PD169316 and MK2 Inhibitor III Activate the Proteasome through Distinct Mechanisms

(A) The structure of MK2 inhibitor III.

(B) In-gel fluorescence scan (top) showing representative proteasome labeling profiles of purified proteasome preparations, obtained from HTBH-Rpn11-HEK293T cells after a 16 hr incubation period with 5 μM of the indicated compounds or after 72 hr transfection with siRNA targeting p38 MAPKα. Bars represent the quantified probe signal. Immunoblot analysis (bottom) of the levels of the indicated proteins. GAPDH levels were used as a loading control.

(C) Suc-LLVY-AMC conversion by purified proteasome preparations, obtained from HTBH-Rpn11-HEK293T cells after a 16 hr incubation period with 5 μM of the indicated proteasome activators or 750 nM MG132 (top). Quantification of substrate turnover (bottom). Error bars represent SD of three independent experiments. Statistical significance: *$p \leq 0.05$, **$p \leq 0.01$, ***$p \leq 0.001$.

(D) Intracellular fluorescence intensities in probe **1**-treated MelJuSo cells after a 16 hr incubation period with the indicated (combinations of) p38 MAPK inhibitors. All signals were normalized to intensities obtained in DMSO-treated control (CTR) cells. Error bars represent SD of three independent experiments.

approach. Following treatment of MelJuSo cells with either inhibitor or DMSO, the 26S proteasome was enriched by affinity purification. Both gel-based proteasome activity assays and measurements of suc-LLVY-AMC conversion confirmed that these proteasome preparations showed increased activity (Figures S4C and S4D). After lysC and trypsin digestion, the purified samples were either subjected to liquid chromatography-tandem mass spectrometry (LC-MS/MS) directly or further subjected to phosphopeptide enrichment using an automated Fe(III)-IMAC approach (Abelin et al., 2016) prior to LC-MS/MS analysis, allowing quantification of phosphorylated proteasomal peptides. Although many known and yet undescribed phosphosites could be detected on these purified proteasomes, no significant differences were found between non-treated cells and cells treated with inhibitors of the p38 MAPK pathway at both total and phosphoprotein levels, including the Rpn2 Thr-273 phosphopeptide (Tables S1 and S2). These data suggest that, although the proteasome can be inhibited through direct phosphorylation, proteasome activation is not necessarily mediated through direct phosphorylation.

We next investigated whether other known mechanisms were involved in the enhancement of proteasome activity through the p38 MAPK pathway inhibition. Increased proteasome subunit transcription and/or translation are among the most common mechanisms of proteasome activation. However, no increase in the mRNA levels of the 20S core subunits PSMB5, PSMB6, and PSMB7 was observed in p38 MAPK inhibitor-treated cells compared with control cells, as determined by real-time PCR (Figure S4E). Moreover, using established 20S subunit ELISA (Heubner et al., 2011) and immunoblot assays, no increase

was detected in the total amount of 20S proteasome or in the level of the 19S RPT6 or 20S β5 subunits, respectively (Figures 2C, S4F, and S4G). The assembly of 19S and 20S particles into 26S proteasome is another mechanism known to increase proteasome activity. To study whether proteasome assembly was affected by p38 MAPK inhibition, we treated MelJuSo cells with PD169316, MK2 inhibitor III, or DMSO, followed by cell lysis. These cells were subsequently fractionated using size-exclusion chromatography and the total amount of proteasome in each fraction was determined by measuring the amounts of subunits specific to the 19S and 20S proteasome using mass spectrometry (Figure S4H). Quantification values of the different 19S or 20S subunits were averaged and plotted against the fraction number. We only analyzed those fractions with LC-MS/MS, in which the proteasome was showing activity, as determined by the gel-based activity assay, and also measured β5 protein levels in these fractions (Figure S4I). Treatment with either inhibitor did not seem to induce a clear shift in elution profile (Figure S4H) and the amount of 19S and 20S proteasome in the fraction containing 26S proteasome (fraction 1) compared with fractions containing the unassembled particles (fractions 5–6 for the 20S proteasome) did not substantially change. Also the proteasome activity profiles and the β5 immunoblots show no changes in the inhibitor-treated cells compared with control cells. In addition, proteomics analyses of proteasome complexes that were immunoprecipitated through HTBH-tagged Rpn11 (a 19S subunit) did not show any significant change in the relative levels of 19S and 20S subunits (Tables S1 and S2). Together with the observation that activated proteasomes retain their activity after purification, these results indicate that inhibition of the p38 pathway likely does not affect proteasome assembly. In addition, proteomics data indicate that neither the levels nor the phosphorylation status of the proteasome activators PSME1-4 or chaperones PSMG1-3, that co-immunoprecipitated with the proteasome, showed any significant change between treatment conditions (Tables S1 and S2). This suggests that proteasome activation is not mediated through differential recruitment of these subunits to the proteasome.

We also asked whether MK2 and p38 MAPK inhibition enhances proteasome activity through distinct mechanisms. To this end, we treated MelJuSo cells with different concentrations of PD169316 and MK2 inhibitor III alone, or in combination at concentrations well below the half maximal inhibitory concentration (IC_{50}) values (Figure S4J), followed by probe **1** labeling and flow cytometry analysis (Figure 4D). Whereas treatment with 0.25 μM PD169316, or 5 or 10 μM MK2 inhibitor III alone, only marginally activated intracellular proteasomes, the combination of both inhibitors at the same sub IC_{50} concentrations enhanced the proteasome activity to near maximal capacity (4-fold activation). Moreover, the concentration of either inhibitor alone needed to reach a similar extent of proteasome activation was 5- to 10-fold higher, suggesting that PD169316 and MK2 inhibitor III operate synergistically in enhancing proteasome activity.

p38 MAPK Inhibition Increases the Degradation of Toxic Protein Assemblies

Finally, we asked whether inhibition of the p38 MAPK pathway and the subsequent activation of the proteasome represents a viable therapeutic strategy to clear toxic protein aggregates associated with many neurodegenerative diseases. Therefore, we first assessed to what extent p38α inhibition can increase proteasome activity. To this end, we depleted p38α from MelJuSo cells using siRNA to maximize proteasome activity, followed by cell lysis. Next, recombinant $p38\alpha^{D176A/F372S}$, a constitutively active mutant of p38α (Avitzour et al., 2007), was added to the lysate in either the presence or absence of PD169316, after which the turnover of suc-LLVY-AMC was measured. Whereas addition of PD169316 alone did not affect the proteasome activity, as expected, supplementation with recombinant $p38\alpha^{D176A/F372S}$ resulted in an over 4-fold reduction in proteasome activity (Figure 5A). Importantly, inhibition of supplemented p38α with PD169316 almost completely restored suc-LLVY-AMC turnover, resulting in an almost 4-fold enhancement of proteasome activity. These results indicate that p38 MAPK inhibition can strongly increase proteasome activity. The effect of p38 MAPK inhibition is especially apparent when basal proteasome activity is low, as has been observed in various neurodegenerative diseases (Dantuma and Bott, 2014; Kristiansen et al., 2007; Rubinsztein, 2006), underscoring the therapeutic promise of this class of compounds.

Next, we monitored the effect of p38 MAPK inhibition on the degradation of both endogenous and overexpressed model protein substrates. The turnover of most proteins, including endogenous estrogen receptor ERα, overexpressed P16, and overexpressed GFP-Bcl-B, was not affected by treatment with proteasome activators, suggesting that the bulk of cellular proteins remain unaltered by proteasome activation. However, p38 MAPK inhibition did result in reduced cellular levels of HA-GFP compared with DMSO-treated control cells (Figure 5B). To examine whether p38 inhibition can also enhance the degradation of ubiquitinated proteins, we used a PROTAC method (Sakamoto et al., 2001). Recently, the compound dBET1 was reported to prompt specific degradation of BRD4 by increasing BRD4 polyubiquitination by the E3 ligase cereblon (CRBN) (Winter et al., 2015). As can be seen in Figure 5C, preincubation with PD169316 enhanced the dBET1-induced degradation of BRD4, without altering the protein levels of CRBN. These results indicate that p38 inhibition can increase the ubiquitin-dependent degradation of proteins.

We also examined whether p38 MAPK inhibition can increase the clearance of toxic protein assemblies by measuring the degradation of overexpressed α-synuclein in a bimolecular fluorescence complementation (BiFC) assay (Outeiro et al., 2008). The protein α-synuclein aggregates to form insoluble fibrils in pathological conditions characterized by Lewy bodies, such as Lewy body dementia and PD. When α-synuclein fused to non-fluorescent split venus fragments is transfected into cells, oligomerization of two α-synuclein proteins causes these non-fluorescent fragments to reconstitute a functional yellow fluorescent protein fluorophore, which can be detected by flow cytometry. Using this BiFC assay, significantly lower levels of α-synuclein assemblies were observed in p38 MAPK inhibitor-treated cells compared with control cells. The levels of co-transfected blue fluorescent protein (BFP) were comparable between all conditions, indicating that p38 MAPK inhibitor treatment does not affect the transcription rate of BFP (Figure 5D). Importantly, the reduction in α-synuclein protein levels was accompanied by an increase in the survival of inhibitor-treated cells (Figure 5D).

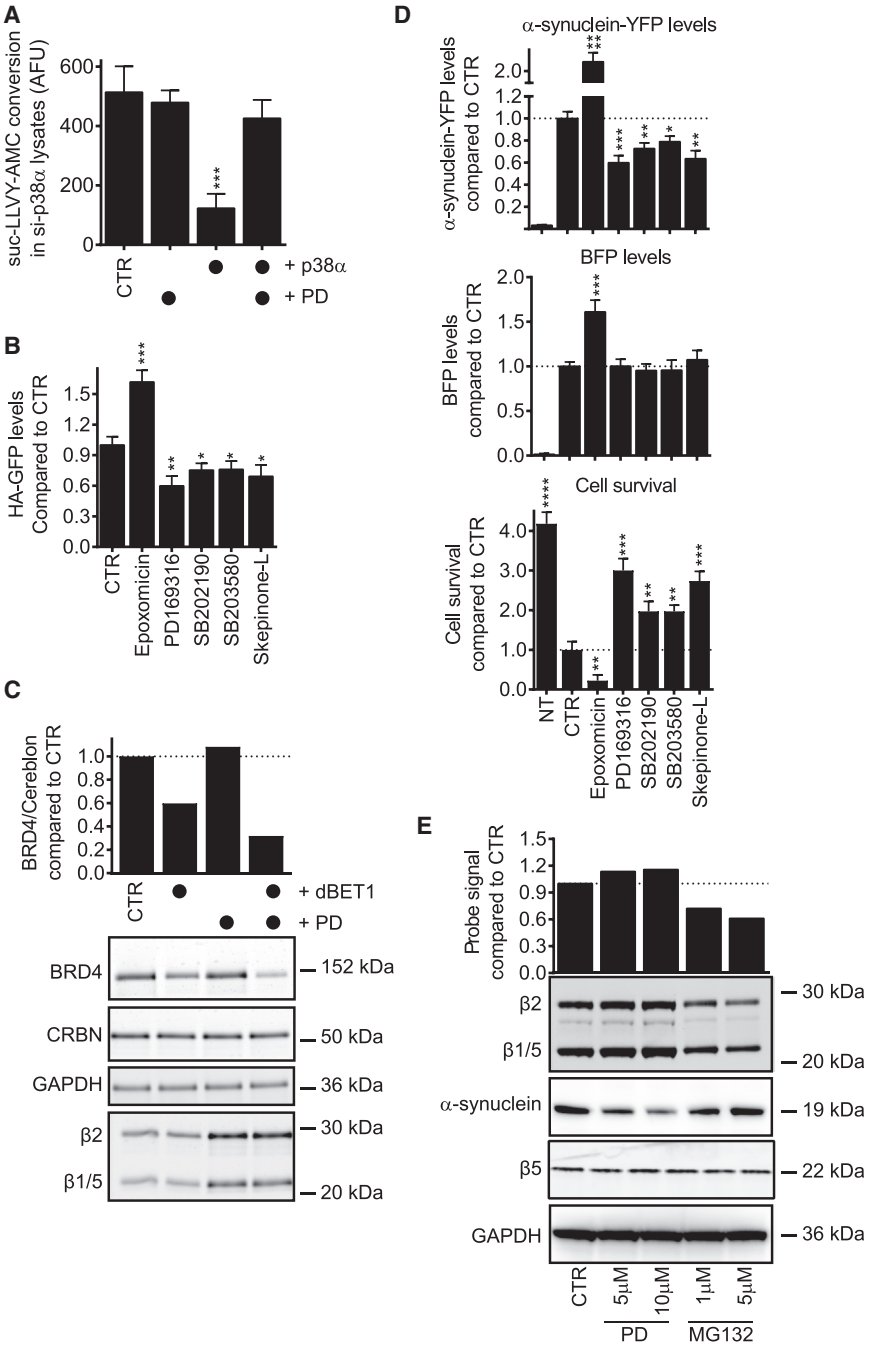

Figure 5. p38 MAPK Inhibition Increases Protein Clearance by the Proteasome

(A) Suc-LLVY-AMC conversion in lysates obtained from MelJuSo cells after 72 hr transfection with siRNAs targeting p38f MAPK. Lysates were subsequently supplemented with a recombinant $p38\alpha^{D176A/F372S}$ protein or its inhibitor PD169316 or a combination of both, before AMC fluorescence measurements were performed. Error bars represent SD of three independent experiments. Statistical significance: ***$p \leq 0.001$.

(B) HA-GFP levels in MelJuSo cells treated with 5 μM of the indicated p38 MAPK inhibitors or epoxomicin. All signals were normalized to intensities obtained in DMSO-treated control (CTR) cells. Error bars represent SD of three independent experiments. Statistical significance: *$p \leq 0.05$, **$p \leq 0.01$, ***$p \leq 0.001$.

(C) Immunoblot analysis showing the levels of the indicated proteins in HeLa cells that were pre-incubated with 5 μM PD169316, followed by a 6 hr treatment with 1 μM dBET1. Bars represent the quantified BRD4/CRBN ratio. Three independent experiments were performed.

(D) α-Synuclein-yellow fluorescent protein (YFP) levels (top), BFP levels (middle) and cell survival (bottom) in MelJuSo cells transfected with α-synuclein-split YFP and BFP and treated with 5 μM of the indicated p38 MAPK inhibitors. All signals were normalized to intensities obtained in DMSO-treated control (CTR) cells. NT, non-transfected. Error bars represent SD of three independent experiments. Statistical significance: *$p \leq 0.05$, **$p \leq 0.01$, ***$p \leq 0.001$ and ****$p \leq 0.0001$.

(E) In-gel fluorescence scan (top) showing representative proteasome labeling profiles in primary mouse neurons after a 16 hr treatment with the indicated concentrations of PD169316 or MG132. Immunoblot analysis (bottom) showing the endogenous α-synuclein, β5 and GAPDH expression levels. GAPDH levels were used as a loading control.

Finally, we tested the effect of PD169316 treatment on endogenous α-synuclein levels in primary mouse neurons. To this end, cells were treated with various concentrations of the drug, after which both the proteasome activity and the levels of α-synuclein were measured. As can be seen in Figure 5E, PD169316 treatment increased the proteasome activity and decreased the levels of endogenous α-synuclein. Together, these data show that inhibition of the p38 MAPK pathway results in an increased clearance of proteins. Furthermore, these data suggest that inhibition of p38 MAPK is a viable strategy to therapeutically enhance proteasome activity, which could contribute to the clearing of protein aggregates in neurodegenerative diseases such as PD.

DISCUSSION

Proteasome activation by small molecules is regarded as a promising strategy to treat or prevent neurodegenerative diseases characterized by the accumulation of toxic protein aggregates (Dantuma and Bott, 2014; Lee et al., 2010a; Myeku et al., 2016). However, very few in vivo small-molecule proteasome enhancers have been described to date. One factor hampering the identification of such compounds is the lack of suitable screening assays. Most proteasome activity assays either work in vitro, or depend on the introduction of tagged substrates to monitor degradation, such as the proteasome reporter substrate Ub-R-GFP (Dantuma et al., 2000). Although such reporter substrates are well suited to monitor proteasome inhibition, their rapid degradation at baseline proteasome activity limits their

use as tools to monitor enhanced activity and degradation. Activity-based proteasome probes overcome these limitations and are therefore powerful research tools to monitor enhancement of 26S proteasome activity in both primary cells and established cell lines and tissues (Berkers et al., 2007). In this study, we identified over ten small molecules that increase 26S proteasome activity in cells using such proteasome activity probes. Our study demonstrates that activity-based probes can be used to identify potent proteasome activators in a straightforward manner.

In addition, our data suggest that proteins in the p38 MAPK pathway are potential targets for therapies aimed at proteasome activation. Genetic and/or chemical inhibition of p38α, its upstream kinases ASK1 and MKK6, and its downstream target MK2 all enhanced proteasome activity in cells. ASK1 and p38 MAPK have previously been shown to negatively regulate the proteasome. Here, we identify the downstream p38 MAPK target MK2 as a novel player that modulates 26S proteasome activity, suggesting that p38α inhibition may activate the 26S proteasome, at least in part, via MK2. Several kinases have been described to modulate proteasome activity through direct phosphorylation of the 19S RP, including ASK1 (Um et al., 2010), p38 MAPK (Lee et al., 2010b), the calcium/calmodulin-dependent protein kinase II (CaMKII) (Djakovic et al., 2009), PKA (Asai et al., 2009; Lokireddy et al., 2015; Zhang et al., 2007), and DYRK2 (Guo et al., 2015). Surprisingly, extensive proteomics studies showed that inhibition of p38 or MK2 did not result in a statistically changed phosphorylation status of the 26S proteasome, although we cannot exclude that the increased proteasomal activity is mediated through (de)phosphorylation of a small fraction of cellular proteasome, without changing global proteasome phosphorylation levels.

The mechanism by which the ten other small-molecule proteasome activators that we identified enhance proteasome activity remains to be determined. Such studies are challenging because of the polypharmacology exhibited by many of these compounds (i.e., these compounds are likely to affect multiple intracellular targets). However, many of these activators have been described to influence Ca^{2+} or cAMP levels in cells. Both CaMKII (Djakovic et al., 2009) and PKA (Asai et al., 2009; Lokireddy et al., 2015; Zhang et al., 2007), which are activated by increased Ca^{2+} and cAMP levels, respectively, have been shown to phosphorylate the proteasome, leading to its activation. Mediating cellular entry of extracellular Ca^{2+} by the small-molecule bicuculline has been shown to stimulate the degradation of proteasomal substrates (Djakovic et al., 2009). In addition, forskolin and other cAMP-inducing compounds promote the degradation of aggregation-prone proteins that cause neurodegenerative disease (Lin et al., 2013; Lokireddy et al., 2015). In vivo, small-molecule-mediated PKA activation enhances 26S proteasome activity, while reducing levels of aggregated tau (Myeku et al., 2016). It therefore seems likely that the proteasome-enhancing properties of some of our other hits are, at least in part, mediated through cAMP or Ca^{2+} signaling. This suggests that the identified set of compounds work through multiple mechanisms in their activation of the proteasome. We expect that elucidation of possible other pathways involved in the regulation of 26S proteasome activity will open up new possibilities for therapy based on 26S proteasome activity modulation.

For most proteasomal substrates, ubiquitination rather than proteasomal degradation is the rate-limiting step in protein breakdown. However, a recent study suggests that the degradation of particularly short-lived proteins, including aggregation-prone proteins, is also regulated at the level of the proteasome (Lokireddy et al., 2015). Our data indicate that p38 MAPK inhibitors indeed do not change global levels of ubiquitinated proteins, indicative of protein turnover, but instead induce the degradation of only a small subset of proteins. Several p38 MAPK inhibitors promote the degradation of endogenous α-synuclein, which (once aggregated) is the causative agent of pathological conditions characterized by Lewy bodies, such as PD. In addition, our data show that these inhibitors increase the clearance of toxic α-synuclein assemblies and rescue cell viability. The reported half-life of endogenous α-synuclein is at least 24 hr (Li et al., 2004), suggesting that increased protein degradation by activated proteasomes is not limited to short-lived proteins only. As activated p38 MAPK has been found to accumulate in various neurodegenerative diseases (Kim and Choi, 2010), proteasome activation via p38 MAPK inhibition may be especially beneficial in neurodegenerative diseases.

SIGNIFICANCE

The 26S proteasome is responsible for the breakdown of cellular proteins and key to protein homeostasis. Many neurodegenerative disorders are characterized by the presence of toxic intracellular protein aggregates and reduced 26S proteasome activity. Here, we describe the identification of more than ten distinct small molecules that increase 26S proteasome activity in cells. One of the identified molecules is a known p38 MAPK inhibitor and we show that chemical inhibition or depletion of p38 MAPK increase PROTACs-mediated degradation of ubiquitinated proteins as well as degradation of α-synuclein, causative to Parkinson's disease. Upon focusing on the MAPK signaling cascade, we further identify a number of additional cellular players along this pathway, including MAPK-activated protein kinase 2, as proteins involved in 26S proteasome activation. Our findings indicate that enhancement of 26S proteasome activity may be of interest as a therapeutic strategy and that such activation can be achieved easier than previously thought.

STAR★METHODS

Detailed methods are provided in the online version of this paper and include the following:

- KEY RESOURCES TABLE
- CONTACT FOR REAGENT AND RESOURCE SHARING
- EXPERIMENTAL MODEL AND SUBJECT DETAILS
  - Cell Culture
- METHOD DETAILS
  - Chemicals
  - Antibodies
  - SiRNAs
  - Plasmids
  - High-Throughput Screening Assays

- Assaying Proteasome Activity Using Proteasome Activity Probe 1 (Flow Cytometry)
- Assaying Proteasome Activity Using Proteasome Activity Probe 1 (SDS-PAGE)
- Assaying Proteasome Activity with Fluorogenic Substrates
- Assaying Proteasome Activity with Fluorescent Reporter Proteins
- PROTAC-Induced Proteolytic Targeting of BRD4
- CellTiter-Blue Cell Viability Assay
- 20S Proteasome ELISA
- Proteasome Isolation
- Real-Time PCR
- Sample Preparation for SEC Proteomics Analysis
- Proteasome Enriched (Phospho)Proteomics Analysis
- Liquid Chromatography and Mass Spectrometry
- Data Processing

● QUANTIFICATION AND STATISTICAL ANALYSIS

SUPPLEMENTAL INFORMATION

Supplemental Information includes four figures and two tables and can be found with this article online at http://dx.doi.org/10.1016/j.chembiol.2017.05.010.

AUTHOR CONTRIBUTIONS

Y.L., A.J., K.W., K.S., B.R., R.P., E.A.Z., B.K., and W.S. performed the experiments. C.R.B. and H.O. managed the study. Y.L., A.J., C.R.B., and H.O. wrote the manuscript. A.R.J.H. and J.B. contributed reagents and analytical tools. S.L. was responsible for the synthesis of skepinone-L.

ACKNOWLEDGMENTS

The authors would like to thank Rob Zwart for technical assistance, Lan Huang for reagents, Koraljka Husnjak for critical reading of the manuscript, Olivier Coux for practical advice, and David Sullivan, Jun Liu, and Curtis Chong for providing us with the Johns Hopkins Clinical Compound Library (JHCCL) version 1.0. This work was supported by a VICI grant to H.O. from the Netherlands Organisation for Scientific Research (NWO) (project 724.013.002). C.R.B. was financially supported by a VENI grant (project 722.013.009) from NWO. R.P. and A.J.R.H. acknowledge NWO-supported large scale proteomics facility Proteins@Work (project 184.032.201) embedded in the Netherlands Proteomic Center.

Received: December 28, 2016
Revised: March 31, 2017
Accepted: May 3, 2017
Published: May 25, 2017

SUPPORTING CITATIONS

The following references appear in the Supplemental Information: Ross et al. (2000).

REFERENCES

Abelin, J.G., Patel, J., Lu, X., Feeney, C.M., Fagbami, L., Creech, A.L., Hu, R., Lam, D., Davison, D., Pino, L., et al. (2016). Reduced-representation phosphosignatures measured by quantitative targeted MS capture cellular states and enable large-scale comparison of drug-induced phenotypes. Mol. Cell Proteomics *15*, 1622–1641.

Al-Ramahi, I., Lam, Y.C., Chen, H.K., de Gouyon, B., Zhang, M., Pérez, A.M., Branco, J., de Haro, M., Patterson, C., Zoghbi, H.Y., et al. (2006). CHIP protects from the neurotoxicity of expanded and wild-type ataxin-1 and promotes their ubiquitination and degradation. J. Biol. Chem. *281*, 26714–26724.

Anderson, D.R., Meyers, M.J., Vernier, W.F., Mahoney, M.W., Kurumbail, R.G., Caspers, N., Poda, G.I., Schindler, J.F., Reitz, D.B., and Mourey, R.J. (2007). Pyrrolopyridine inhibitors of mitogen-activated protein kinase-activated protein kinase 2 (MK-2). J. Med. Chem. *50*, 2647–2654.

Asai, M., Tsukamoto, O., Minamino, T., Asanuma, H., Fujita, M., Asano, Y., Takahama, H., Sasaki, H., Higo, S., Asakura, M., et al. (2009). PKA rapidly enhances proteasome assembly and activity in in vivo canine hearts. J. Mol. Cell Cardiol. *46*, 452–462.

Atzori, C., Ghetti, B., Piva, R., Srinivasan, A.N., Zolo, P., Delisle, M.B., Mirra, S.S., and Migheli, A. (2001). Activation of the JNK/p38 pathway occurs in diseases characterized by tau protein pathology and is related to tau phosphorylation but not to apoptosis. J. Neuropathol. Exp. Neurol. *60*, 1190–1197.

Avitzour, M., Diskin, R., Raboy, B., Askari, N., Engelberg, D., and Livnah, O. (2007). Intrinsically active variants of all human p38 isoforms. FEBS J. *274*, 963–975.

Bendotti, C., Atzori, C., Piva, R., Tortarolo, M., Strong, M.J., DeBiasi, S., and Migheli, A. (2004). Activated p38MAPK is a novel component of the intracellular inclusions found in human amyotrophic lateral sclerosis and mutant SOD1 transgenic mice. J. Neuropathol. Exp. Neurol. *63*, 113–119.

Benjamini, Y., and Hochberg, Y. (1995). Controlling the false discovery rate: a practical and powerful approach to multiple testing. J. R. Stat. Soc. Ser. B (Methodological) *57*, 289–300.

Berkers, C.R., Verdoes, M., Lichtman, E., Fiebiger, E., Kessler, B.M., Anderson, K.C., Ploegh, H.L., Ovaa, H., and Galardy, P.J. (2005). Activity probe for in vivo profiling of the specificity of proteasome inhibitor bortezomib. Nat. Methods *2*, 357–362.

Berkers, C.R., van Leeuwen, F.W., Groothuis, T.A., Peperzak, V., van Tilburg, E.W., Borst, J., Neefjes, J.J., and Ovaa, H. (2007). Profiling proteasome activity in tissue with fluorescent probes. Mol. Pharm. *4*, 739–748.

Borst, O., Walker, B., Münzer, P., Russo, A., Schmid, E., Faggio, C., Bigalke, B., Laufer, S., Gawaz, M., and Lang, F. (2013). Skepinone-L, a novel potent and highly selective inhibitor of p38 MAP kinase, effectively impairs platelet activation and thrombus formation. Cell Physiol. Biochem. *31*, 914–924.

Dahlmann, B., Ruppert, T., Kuehn, L., Merforth, S., and Kloetzel, P.M. (2000). Different proteasome subtypes in a single tissue exhibit different enzymatic properties. J. Mol. Biol. *303*, 643–653.

Dantuma, N.P., and Bott, L.C. (2014). The ubiquitin-proteasome system in neurodegenerative diseases: precipitating factor, yet part of the solution. Front. Mol. Neurosci. *7*, 70.

Dantuma, N.P., Lindsten, K., Glas, R., Jellne, M., and Masucci, M.G. (2000). Short-lived green fluorescent proteins for quantifying ubiquitin/proteasome-dependent proteolysis in living cells. Nat. Biotechnol. *18*, 538–543.

de Jong, A., Schuurman, K.G., Rodenko, B., Ovaa, H., and Berkers, C.R. (2012). Fluorescence-based proteasome activity profiling. Methods Mol. Biol. *803*, 183–204.

de Wit, J., Toonen, R.F., and Verhage, M. (2009). Matrix-dependent local retention of secretory vesicle cargo in cortical neurons. J. Neurosci. *29*, 23–37.

Djakovic, S.N., Schwarz, L.A., Barylko, B., DeMartino, G.N., and Patrick, G.N. (2009). Regulation of the proteasome by neuronal activity and calcium/calmodulin-dependent protein kinase II. J. Biol. Chem. *284*, 26655–26665.

Ebrahimi-Fakhari, D., Cantuti-Castelvetri, I., Fan, Z., Rockenstein, E., Masliah, E., Hyman, B.T., McLean, P.J., and Unni, V.K. (2011). Distinct roles in vivo for the ubiquitin-proteasome system and the autophagy-lysosomal pathway in the degradation of α-synuclein. J. Neurosci. *31*, 14508–14520.

Glickman, M.H., and Ciechanover, A. (2002). The ubiquitin-proteasome proteolytic pathway: destruction for the sake of construction. Physiol. Rev. *82*, 373–428.

Guo, X., Wang, X., Wang, Z., Banerjee, S., Yang, J., Huang, L., and Dixon, J.E. (2015). Site-specific proteasome phosphorylation controls cell proliferation and tumorigenesis. Nat. Cell Biol. *18*, 202–212.

Heubner, M., Wimberger, P., Dahlmann, B., Kasimir-Bauer, S., Kimmig, R., Peters, J., Wohlschlaeger, J., and Sixt, S.U. (2011). The prognostic impact of circulating proteasome concentrations in patients with epithelial ovarian cancer. Gynecol. Oncol. *120*, 233–238.

Hideshima, T., Richardson, P., Chauhan, D., Palombella, V.J., Elliott, P.J., Adams, J., and Anderson, K.C. (2001). The proteasome inhibitor PS-341 inhibits growth, induces apoptosis, and overcomes drug resistance in human multiple myeloma cells. Cancer Res. *61*, 3071–3076.

Kim, E.K., and Choi, E.J. (2010). Pathological roles of MAPK signaling pathways in human diseases. Biochim. Biophys. Acta *1802*, 396–405.

Kniepert, A., and Groettrup, M. (2014). The unique functions of tissue-specific proteasomes. Trends Biochem. Sci. *39*, 17–24.

Koeberle, S.C., Romir, J., Fischer, S., Koeberle, A., Schattel, V., Albrecht, W., Grütter, C., Werz, O., Rauh, D., Stehle, T., et al. (2012). Skepinone-L is a selective p38 mitogen-activated protein kinase inhibitor. Nat. Chem. Biol. *8*, 141–143.

Köhler, A., Cascio, P., Leggett, D.S., Woo, K.M., Goldberg, A.L., and Finley, D. (2001). The axial channel of the proteasome core particle is gated by the Rpt2 ATPase and controls both substrate entry and product release. Mol. Cell *7*, 1143–1152.

Kristiansen, M., Deriziotis, P., Dimcheff, D.E., Jackson, G.S., Ovaa, H., Naumann, H., Clarke, A.R., van Leeuwen, F.W., Menéndez-Benito, V., Dantuma, N.P., et al. (2007). Disease-associated prion protein oligomers inhibit the 26S proteasome. Mol. Cell *26*, 175–188.

Lee, F.K., Wong, A.K., Lee, Y.W., Wan, O.W., Chan, H.Y., and Chung, K.K. (2009). The role of ubiquitin linkages on alpha-synuclein induced-toxicity in a *Drosophila* model of Parkinson's disease. J. Neurochem. *110*, 208–219.

Lee, B.H., Lee, M.J., Park, S., Oh, D.C., Elsasser, S., Chen, P.C., Gartner, C., Dimova, N., Hanna, J., Gygi, S.P., et al. (2010a). Enhancement of proteasome activity by a small-molecule inhibitor of USP14. Nature *467*, 179–184.

Lee, S.H., Park, Y., Yoon, S.K., and Yoon, J.B. (2010b). Osmotic stress inhibits proteasome by p38 MAPK-dependent phosphorylation. J. Biol. Chem. *285*, 41280–41289.

Li, W., Lesuisse, C., Xu, Y., Troncoso, J.C., Price, D.L., and Lee, M.K. (2004). Stabilization of alpha-synuclein protein with aging and familial Parkinson's disease-linked A53T mutation. J. Neurosci. *24*, 7400–7409.

Li, X., and Demartino, G.N. (2009). Variably modulated gating of the 26S proteasome by ATP and polyubiquitin. Biochem. J. *421*, 397–404.

Lin, J.T., Chang, W.C., Chen, H.M., Lai, H.L., Chen, C.Y., Tao, M.H., and Chern, Y. (2013). Regulation of feedback between protein kinase A and the proteasome system worsens Huntington's disease. Mol. Cell Biol. *33*, 1073–1084.

Liu, Y., Hettinger, C.L., Zhang, D., Rezvani, K., Wang, X., and Wang, H. (2014). Sulforaphane enhances proteasomal and autophagic activities in mice and is a potential therapeutic reagent for Huntington's disease. J. Neurochem. *129*, 539–547.

Lokireddy, S., Kukushkin, N.V., and Goldberg, A.L. (2015). cAMP-induced phosphorylation of 26S proteasomes on Rpn6/PSMD11 enhances their activity and the degradation of misfolded proteins. Proc. Natl. Acad. Sci. USA *112*, E7176–E7185.

Myeku, N., Clelland, C.L., Emrani, S., Kukushkin, N.V., Yu, W.H., Goldberg, A.L., and Duff, K.E. (2016). Tau-driven 26S proteasome impairment and cognitive dysfunction can be prevented early in disease by activating cAMP-PKA signaling. Nat. Med. *22*, 46–53.

Outeiro, T.F., Putcha, P., Tetzlaff, J.E., Spoelgen, R., Koker, M., Carvalho, F., Hyman, B.T., and McLean, P.J. (2008). Formation of toxic oligomeric alpha-synuclein species in living cells. PLoS One *3*, e1867.

Pelletier, S., Schuurman, K.G., Berkers, C.R., Ovaa, H., Heck, A.J., and Raijmakers, R. (2010). Quantifying cross-tissue diversity in proteasome complexes by mass spectrometry. Mol. Biosyst. *6*, 1450–1453.

Perrotton, T., Trompier, D., Chang, X.B., Di Pietro, A., and Baubichon-Cortay, H. (2007). (R)- and (S)-verapamil differentially modulate the multidrug-resistant protein MRP1. J. Biol. Chem. *282*, 31542–31548.

Peth, A., Besche, H.C., and Goldberg, A.L. (2009). Ubiquitinated proteins activate the proteasome by binding to Usp14/Ubp6, which causes 20S gate opening. Mol. Cell *36*, 794–804.

Ross, D.T., Scherf, U., Eisen, M.B., Perou, C.M., Rees, C., Spellman, P., Iyer, V., Jeffrey, S.S., Van de Rijn, M., Waltham, M., et al. (2000). Systematic variation in gene expression patterns in human cancer cell lines. Nat. Genet. *24*, 227–235.

Rubinsztein, D.C. (2006). The roles of intracellular protein-degradation pathways in neurodegeneration. Nature *443*, 780–786.

Sakamoto, K.M., Kim, K.B., Kumagai, A., Mercurio, F., Crews, C.M., and Deshaies, R.J. (2001). Protacs: chimeric molecules that target proteins to the Skp1-Cullin-F box complex for ubiquitination and degradation. Proc. Natl. Acad. Sci. USA *98*, 8554–8559.

Snyder, H., Mensah, K., Theisler, C., Lee, J., Matouschek, A., and Wolozin, B. (2003). Aggregated and monomeric alpha-synuclein bind to the S6' proteasomal protein and inhibit proteasomal function. J. Biol. Chem. *278*, 11753–11759.

Tortarolo, M., Veglianese, P., Calvaresi, N., Botturi, A., Rossi, C., Giorgini, A., Migheli, A., and Bendotti, C. (2003). Persistent activation of p38 mitogen-activated protein kinase in a mouse model of familial amyotrophic lateral sclerosis correlates with disease progression. Mol. Cell Neurosci. *23*, 180–192.

Tsai, Y.C., Fishman, P.S., Thakor, N.V., and Oyler, G.A. (2003). Parkin facilitates the elimination of expanded polyglutamine proteins and leads to preservation of proteasome function. J. Biol. Chem. *278*, 22044–22055.

Tyanova, S., Temu, T., Sinitcyn, P., Carlson, A., Hein, M.Y., Geiger, T., Mann, M., and Cox, J. (2016). The Perseus computational platform for comprehensive analysis of (prote)omics data. Nat. Methods *13*, 731–740.

Um, J.W., Im, E., Park, J., Oh, Y., Min, B., Lee, H.J., Yoon, J.B., and Chung, K.C. (2010). ASK1 negatively regulates the 26 S proteasome. J. Biol. Chem. *285*, 36434–36446.

Wang, X., Chen, C.F., Baker, P.R., Chen, P.L., Kaiser, P., and Huang, L. (2007). Mass spectrometric characterization of the affinity-purified human 26S proteasome complex. Biochemistry *46*, 3553–3565.

Winter, G.E., Buckley, D.L., Paulk, J., Roberts, J.M., Souza, A., Dhe-Paganon, S., and Bradner, J.E. (2015). DRUG DEVELOPMENT. Phthalimide conjugation as a strategy for in vivo target protein degradation. Science *348*, 1376–1381.

Zhang, F., Hu, Y., Huang, P., Toleman, C.A., Paterson, A.J., and Kudlow, J.E. (2007). Proteasome function is regulated by cyclic AMP-dependent protein kinase through phosphorylation of Rpt6. J. Biol. Chem. *282*, 22460–22471.

Zhou, H., Ye, M., Dong, J., Corradini, E., Cristobal, A., Heck, A.J., Zou, H., and Mohammed, S. (2013). Robust phosphoproteome enrichment using monodisperse microsphere-based immobilized titanium (IV) ion affinity chromatography. Nat. Protoc. *8*, 461–480.

Zhu, X., Rottkamp, C.A., Boux, H., Takeda, A., Perry, G., and Smith, M.A. (2000). Activation of p38 kinase links tau phosphorylation, oxidative stress, and cell cycle-related events in Alzheimer disease. J. Neuropathol. Exp. Neurol. *59*, 880–888.

STAR★METHODS

KEY RESOURCES TABLE

REAGENT or RESOURCE	SOURCE	IDENTIFIER
Antibodies		
Rpt6	Enzo Lifesciences	Cat# BML-PW9265; RRID: AB_10555017
β5 (PSMB5)	Enzo Lifesciences	Cat# BML-PW8895; RRID: AB_10540901
P38 MAPK	Enzo Lifesciences	Cat# ADI-KAS-MA009; RRID: AB_11026937
ASK1	Abcam	Cat# AB45178; RRID: AB_722915
MKK6	Enzo Lifesciences	Cat# ADI-KAP-MA014; RRID: AB_10617283
MAPKAPK2	Cell Signaling Technologies	Cat# 3042; RRID: AB_10694238
α-synuclein	BD Transduction Laboratories	Cat# 610787; RRID: AB_398108
Ubiquitin	Santa Cruz Biotechnology	Cat# SC-8017; RRID: AB_628423
GAPDH	Life Technologies	Cat# AM4300; RRID: AB_2536381
BRD4	Abcam	Cat# AB128874; RRID: AB_11145462
CRBN	Abcam	Cat# AB98992; RRID: AB_10674459
HRP-conjugated polyclonal swine anti-rabbit	DAKO	Cat# P0217
HRP-conjugated polyclonal rabbit anti-mouse	DAKO	Cat# P0161
Chemicals, Peptides, and Recombinant Proteins		
Cyclosporin A (CycA)	Sigma Aldrich	C30024
Dipyrimadole (Dip)	Sigma Aldrich	D9766
DPCPX (DP)	Sigma Aldrich	C101
Loperamide (Lop)	Sigma Aldrich	L4762
Methylbenzethonium (MB)	Sigma Aldrich	M7379
Mifepristone (Mif)	Sigma Aldrich	M8046
PD169316	Sigma Aldrich	P9248
Pimozide (Pim)	Sigma Aldrich	P1793
Proflavine (Pro)	Sigma Aldrich	P2508
(±)-Verapamil (Ver)	Sigma Aldrich	V105
Win 62,577 (Win)	Sigma Aldrich	W104
SB202190	Sigma Aldrich	S7067
SB203580	Sigma Aldrich	S8307
Skepinone-L	Stefan Laufer (Koeberle et al., 2012)	N/A
IU1	Lee et al., 2010a	I1911
dBET1	BioMol	Cay18044-1
Probe 1: Me_4-BodipyFLAhx$_3$Leu$_3$VS	de Jong et al., 2012	N/A
Reduced probe 1	Berkers et al., 2005	N/A
Suc-Leu-Leu-Val-Tyr-AMC	Enzo Lifesciences	BML-P802
PhoSTOP	Roche	4906845001
cOmplete Protease EDTA-free Protease Inhibitor cocktail	Roche	4693159001
Critical Commercial Assays		
Proteasome ELISA kit	Enzo Lifesciences	BML-PW0575-0001
CellTiter-Blue Cell Viability Assay	Promega	G8080
Dynabeads mRNA DIRECT Purification kit	Thermo Fischer Scientific	61011
SuperScript VILO cDNA Synthesis kit	Thermo Fischer Scientific	11754250
SYBRgreen PCR Master Mix	Applied Biosciences	4309155
Gel Filtration Markers Kit for Protein Molecular Weights 6,500-66,000 Da	Sigma Aldrich	MWGF70

(*Continued on next page*)

Continued

REAGENT or RESOURCE	SOURCE	IDENTIFIER
Experimental Models: Cell Lines		
Human: HEK293T cells stably expressing HTBH-tagged Rpn11	Lan Huang (University of California, Irvine)	N/A
Human: MelJuSo	Division of Chemical Immunology, LUMC, Leiden	N/A
Human: MCF-7	Division of Chemical Immunology, LUMC, Leiden	N/A
Human: HEK293	Division of Chemical Immunology, LUMC, Leiden	N/A
Human: HeLa	Division of Chemical Immunology, LUMC, Leiden	N/A
Human: THP-1	Division of Chemical Immunology, LUMC, Leiden	N/A
Experimental Models: Organisms/Strains		
Primary mouse neurons	Wiep Scheper (de Wit et al., 2009)	N/A
Oligonucleotides		
siRNA P38α (MAPK14)	Sigma Aldrich	SIHK1201, SIHK1202, SIHK1203
siRNA P38β (MAPK11)	Sigma Aldrich	SIHK1192, SIHK1193, SIHK1194
siRNA P38γ (MAPK12)	Sigma Aldrich	SIHK1195 SIHK1196, SIHK1197,
siRNA P38δ (MAPK13)	Sigma Aldrich	SIHK1198, SIHK1199, SIHK1200
siRNA ASK1	Dharmacon	M-003584-02
siRNA MKK6	Dharmacon	M-003967-01
siRNA MK2	Dharmacon	M-003516-02
siRNA PLK1	Dharmacon	M-003290-01
siRNA Nontargeting	Dharmacon	D-001206-13 D-001206-14
Primer PSMB5 Forward 5'-CTTCAAGTTCCGCCATGGA-3' Reverse 5'-CCGTCTGGGAGGCAATGTAA-3'	Thermo Fisher Scientific	N/A
Primer PSMB6 Forward 5'-AGGCATGACCAAGGA-AGAGTGT-3' Reverse 5'-GAGCCATCCCGCTCCAT-3'	Thermo Fisher Scientific	N/A
Primer PSMB7 Forward 5'-TCGGTGTATGCTCCACCAGTT-3' Reverse 5'-GCAAAATCGGCTT-CCAAGAC-3'	Thermo Fisher Scientific	N/A
Primer P38α (MAPK14) Forward 5'-AAGACTCGTTGGAACCCCAG-3' Reverse 5'-TCCAGTAGGTCGAC-AGCCAG-3'	Thermo Fisher Scientific	N/A
Primer P38β (MAPK11) Forward 5'-AGCCCAGTGTCCCTCCTAA-3' Reverse 5'-CCACAGGCAACCACAAATCT-3'	Thermo Fisher Scientific	N/A
Primer P38γ (MAPK12) Forward 5'-AGCCCTCAGGCTGTGAATCT-3' Reverse 5'-CATATTTCTGGGCCT-TGGGT-3'	Thermo Fisher Scientific	N/A
Primer P38δ (MAPK13) Forward 5'-GCTCACCCCTTCTTTGAACC-3' Reverse 5'-TTCGTCCACGCTGAGTTTCT-3'	Thermo Fisher Scientific	N/A
Primer GUS Forward 5'-GAAAATATGTGGTTGGAGAGCTCATT-3' Reverse 5'-CCGAGTGAAGATCCCCTTTTTA-3'	Thermo Fisher Scientific	N/A

(*Continued on next page*)

Continued

REAGENT or RESOURCE	SOURCE	IDENTIFIER
Recombinant DNA		
Plasmids: α-synuclein BIFC assay	Tiago Outeiro (Outeiro et al., 2008)	N/A
Plasmid: p38 MAPα$^{D176A/F372S}$	Avitzour et al., 2007	N/A
Plasmid: (GY)HA-GFP	Jannie Borst	N/A
Plasmid: Blue Fluorescent Protein (BFP)	Jannie Borst	N/A
Software and Algorithms		
GraphPad Prism	Graphpad Software Inc	https://www.graphpad.com/scientific-software/prism/
FlowJo	Tree Star	https://www.flowjo.com/
Max Quant (v1.5.2.8)	N/A	http://www.coxdocs.org/doku.php?id=maxquant:start
Perseus (v1.5.0.0	Tyanova et al., 2016	http://www.coxdocs.org/doku.php?id=perseus:start
ImageQuant TL 8.1	GE Healthcare Life Sciences	http://www.gelifesciences.com/webapp/wcs/stores/servlet/ProductDisplay?categoryId=10988&catalogId=10101&productId=25675&storeId=12251&langId=-1

CONTACT FOR REAGENT AND RESOURCE SHARING

Further information and requests for resources and reagents should be directed to and will be fulfilled by the Lead Contact, Huib Ovaa (H.Ovaa@lumc.nl)

EXPERIMENTAL MODEL AND SUBJECT DETAILS

Cell Culture

MelJuSo (human, melanoma), MCF-7 (human, breast adenocarcinoma), HEK293 (human embryonic kidney), and HeLa (human, cervical adenocarcinoma) cells were cultured in DMEM medium (Invitrogen Life Technologies, Carlsbad, CA, USA). THP-1 cells (human, acute monocytic leukemia) were cultured in RPMI medium (Invitrogen Life Technologies, Carlsbad, CA, USA). All media were supplemented with 10% fetal calf serum (Gibco), 100 units/mL penicillin and 100 μg/mL streptomycin. All cells were routinely tested for *Mycoplasma* contaminations. Primary mouse neurons were isolated and differentiated as previously described (de Wit et al., 2009). In brief: cerebral cortices were dissected in Hanks Balanced Salt Solution (HBSS) and digested with 0.25% trypsin (Invitrogen Life Technologies, Carlsbad, CA, USA) for 20 minutes at 37°C. Tissue was triturated, counted and 200.000 neurons per well were plated in a 6-well plate and cultured in Neurobasal medium supplemented with 2% B-2, 1.8% HEPES, 1% glutaMAX (Thermo Fischer Scientific, and 100 units/mL penicillin and 100 μg/mL streptomycin (Invitrogen Life Technologies, Carlsbad, CA, USA). Treatment with compounds was started after 7 days of in vitro culturing. HEK293T cells stably expressing HTBH-tagged Rpn11 were kindly provided by Lan Huang (University of California, Irvine).

METHOD DETAILS

Chemicals

Proteasome activity probe **1** was obtained as described previously (de Jong et al., 2012). Reduced probe **1** was generated by hydrogenation of the vinyl sulfone warhead by Pd/C-H_2 catalysis, as previously described (Berkers et al., 2005), before coupling to the Me_4-BodipyFLAhx$_3$Leu$_3$OH as described previously (de Jong et al., 2012). The Library of Pharmacologically Active Compounds (LOPAC, Lot No. 067K4707) contains 1261 pharmacologically active compounds and was purchased from Sigma-Aldrich. The Johns Hopkins Chemical Compound Library v1.1 (JHCCL) contains 1514 approved drugs and was provided by John Hopkins University. Unless stated otherwise, all compounds were purchased from Sigma-Aldrich at the highest available purity. dBET1 was purchased from Biomol. The allosteric p38 MAPK inhibitor Skepinone–L was previously described (Koeberle et al., 2012) and was kindly provided by Stefan Laufer.

Antibodies

The following primary antibodies were used: Rpt6 (Enzo Lifesciences, BML-PW9265, 1:2000), β5 (PSMB5) (Enzo Lifesciences, BML-PW8895, 1: 2500), p38 MAPK (Enzo Lifesciences, ADI-KAS-MA009, 1:1000), ASK1 (Abcam, AB45178, 1:500), MKK6 (Enzo

Lifesciences, ADI-KAP-MA014, 1:1000), MK2 (Cell Signaling Technologies, #3042, 1:1000), α-synuclein (BD Transduction Laboratories, 610787, 1:1000), ubiquitin (Santa Cruz Biotechnology, SC-8017, 1:1000), BRD4 (Abcam, AB128874, 1:1000), CRBN (Abcam, AB98992, 1:1500), and GAPDH (Life Technologies, AM4300, 1:2500). The following secondary antibodies were used: HRP-conjugated polyclonal swine anti-rabbit (DAKO, P0217) and HRP-conjugated polyclonal rabbit anti-mouse (DAKO, P0161).

SiRNAs

For the siRNA screen, a subset of the GE Healthcare Dharmacon RNAi smartpool library (Dharmacon, Lafayette, CO, USA) was used. For both validation of hits and further assays, siRNAs were obtained from Sigma-Aldrich: P38α (MAPK14): SIHK1201, SIHK1202, siHK1203. P38β (MAPK11): SIHK1192, SIHK1193, SIHK1194. P38γ (MAPK12): SIHK1195, SIHK1196, SIHK1197. P38δ (MAPK13): SIHK1198, SIHK1199, SIHK1200). The following siRNAs were obtained from Dharmacon: ASK1 M-003584-02, MKK6: M-003967-01. MK2: M-003516-02. As a control, cells were transfected with non-targeting siRNAs D-001206-13 or D-001206-14. To determine transfection efficiency, cells were transfected with siRNA against PLK1: M-003290-01.

Plasmids

The construct encoding the constitutively active p38 MAPαD176A/F372S mutant was previously described (Avitzour et al., 2007). Constructs encoding the α-synuclein BiFC assay (Outeiro et al., 2008) were previously described and kindly provided by Tiago Outeiro. Constructs for (GY)HA-GFP and BFP were provided by the Division of Immunology, The Netherlands Cancer Institute, Amsterdam, The Netherlands and previously described.

High-Throughput Screening Assays

All screens were performed on a Hamilton STAR R&D liquid handling system (Hamilton, Reno, NV, USA). For the small molecule screens, MelJuSo cells were grown to 40% confluency in 96-well plates and incubated with 5 μM compound for 16 hours, followed by active proteasome labeling with 250 nM probe **1** for 2 hours. For the siRNA screen, MelJuSo cells were reverse transfected for 48 hours by seeding cells in 96-well plates preprinted with siRNAs, followed by labeling with 250 nM probe **1** for 2 hours. After labeling, cells were washed, trypsinized and fixed with 1% formaldehyde in PBS. The fluorescence in the FL-1 channel (530/30 nm) was measured using a BD FACScalibur (BD Biosciences, San Jose, CA, USA) equipped with an autosampler. For both screens, samples were measured in duplicate.

Assaying Proteasome Activity Using Proteasome Activity Probe 1 (Flow Cytometry)

For small molecule assays, the adherent cell lines MelJuSo, HeLa, MCF-7, N2A and the suspension cell line THP-1 were incubated with 5 μM compound for 16 hours, followed by labeling with 250 nM probe **1** or control probe **1** for 2 hours. Adherent cells were approximately 40% confluent at the start of the incubation. For THP-1 cells approximately 500.000 cells were used. After labeling, cells were washed, trypsinized and fixed with 1% formaldehyde in PBS. The fluorescence in the FL-1 channel (530/30 nm) was measured using a BD FACScalibur (BD Biosciences, San Jose, CA, USA) equipped with an autosampler. Cells treated with DMSO only or 750 nM MG132 were used as untreated or negative controls, respectively. Three independent experiments measured in triplicate were performed. Fluorescence data were normalized by setting the DMSO only-treated samples as 1. For siRNA assays, MelJuSo cells at an approximate confluency of 30% were transfected for 48 hours with 25 nM siRNA listed above using DharmaFECT 1 as transfection reagent, followed by labeling with 250 nM probe **1** for 2 hours. After labeling, cells were washed, trypsinized and fixed with 1% formaldehyde in PBS. The fluorescence in the FL-1channel (530/30 nm) was measured using a BD FACScalibur (BD Biosciences, San Jose, CA, USA) equipped with an autosampler. Cells transfected with non-targeting siRNA were used as untreated control and transfection efficiency was verified by using cells transfected with siRNA against PLK-1. Fluorescence data were normalized by setting the non-targeting siRNA-treated samples as 1. Three independent experiments measured in triplicate were performed.

Assaying Proteasome Activity Using Proteasome Activity Probe 1 (SDS-PAGE)

Cells were treated with compounds as described above. After labeling, cells were harvested and resuspended in HR buffer (50 mM Tris, 5 mM $MgCl_2$, 250 mM sucrose, 1 mM DTT and 2 mM ATP, pH=7.4). Cell lysis was achieved by sonication (Bioruptor, Diagenode, high intensity for 5 minutes with an ON/OFF cycle of 30 seconds) at 4°C. After a centrifugation step (21.100g for 15 minutes) to remove cell debris, protein concentration of the supernatant was determined by a NanoDrop spectrophotometer (Thermo Fisher Scientific) by measuring the absorbance at 280 nm. Equal amounts of protein were denatured by boiling in LDS (lithium dodecyl sulfate) sample buffer (Invitrogen Life Technologies, Carlsbad, CA, USA) containing 2.5% β-mercaptoethanol. Polypeptides were resolved by 12% SDS-PAGE using the NuPAGE system and MOPS running buffer (Invitrogen Life Technologies, Carlsbad, CA, USA). Wet gel slabs were imaged for 60 seconds, with a resolution of 100 μm, using the ProXPRESS 2D Proteomic imaging system (Perkin-Elmer), with appropriate filter settings (λ(ex/em) =480/530 nm). To verify equal protein loading, gels were stained with Coomassie brilliant blue (CBB). For Western Blot analysis, proteins were transferred onto PVDF membrane using the Trans-Blot Semi-Dry Transfer Cell (Bio-Rad). Proteins were transferred at 12 V for 50 minutes. Membranes were blocked with 5% BSA solution and subsequently incubated with primary antibody overnight at 4°C. After washing with PBS-Tween 20 (0.2%) membranes were incubated with secondary antibody and signals visualized by using a Bio-Rad ChemiDoc Imaging System. Immunoblotting with an antibody against GADPH was used to verify equal protein loading. Three independent experiments were performed.

Assaying Proteasome Activity with Fluorogenic Substrates

An equal amount of MelJuSo wild-type cells were seeded in a 96-wells plate. After overnight culturing cells were approximately 40% confluent and were treated with 5 μM compound for 16 hours unless indicated otherwise. Cells were then washed with PBS and 100 μL of assay buffer (20 mM Tris, 5 mM MgCl2, 1 mM DTT, 1 mM ATP, pH=7.4) containing 100 μM suc-LLVY-AMC (Enzo Lifesciences) was added to the cells. Fluorescence was measured every 5 minutes for 50 minutes at 37°C using a Fluostar Optima 96-well plate reader (BMG Labtechnologies; λex / em) = 355 / 450 nm), and the increase in fluorescence per minute was used to calculate the activity of each sample compared to DMSO only-treated cell (100%) and cells treated with 1 μM epoxomicin (0%). Three independent experiments measured in triplicate were performed. Data were analyzed and statistical analyses performed using GraphPad Prism software (GraphPad, La Jolla, CA, USA). To exclude the possibility that the observed results were the consequence of differences in cell number, cell density was subsequently measured. For assaying proteasome activity with fluorescent substrates after siRNA transfection, the following approach was used: MelJuSo cells transfected for 48 hours with either non-targeting siRNA or siRNA targeting p38MAPKα, ASK1, MKK6 or MK2 were washed, trypsinized and counted. For each condition equal amounts of cells were seeded in a 96-wells plate and cultured for additional 6 hours. Cells were washed with PBS and suc-LLVY-AMC conversion was determined as described above. The activity of samples treated with non-targeting siRNA was set as a 100%. After the fluorescent measurement cells were harvested and a Western blot analysis performed to verify knockdown of the respective proteins. To assay the activity of isolated 26S proteasomes (described below) from HEK293T cells stably expressing HTBH-tagged Rpn11, 1 μg of isolated 26S proteins was transferred to a 96-wells plate after which 100 μL of assay buffer was added and the fluorescence measured as described above.

Assaying Proteasome Activity with Fluorescent Reporter Proteins

MelJuSo cells were plated 24 hours, growing to 30–40% confluency prior to transfection. Transfection was performed using Superfect reagent (Qiagen, Chatsworth, CA, USA) according to the manufacturer's instructions and as previously described (31). Cells were transfected with 0.02 μg DNA for (GY)HA-GFP or 0.02 μg of each of the plasmid for α-synuclein. After 48 hours, the compounds were added at the indicated concentrations for 16 hours, after which the fluorescence was measured in the FL-1 channel (530/30 nm using a BD LSRFortessa (BD Biosciences, San Jose, CA, USA). Three independent experiments measured in triplicate were performed.

PROTAC-Induced Proteolytic Targeting of BRD4

HeLa cells were plated 24 hours, growing to 30-40% confluency prior to treatment with either DMSO or 5 μM PD169316 for 16 hours. PROTAC-induced proteolytic targeting of BRD4 (Winter et al., 2015) was induced by treating cells with 1 μM of dBET1 for 6 hours, followed by labeling with 250 nM probe **1** for 2 hours. Fluorescence scanning and immunoblotting was performed as described above to determine the levels of proteasome activity, BRD4 and Cereblon (CRBN). Immunoblotting with an antibody against GADPH was used to verify equal protein loading. Three independent experiments were performed.

CellTiter-Blue Cell Viability Assay

Cells (20% confluent) were incubated with 5 μM compound for 72 hours, followed by incubation with the Cell-Titer-Blue assay reagent (Promega) according to the manufacturer's instruction. The increase in fluorescence (544 nm excitation and 590 nm emission) was measured after 8 hours using an EnVision plate reader (Perkin-Elmer). All results were expressed as a percentage relative to a DMSO-treated control. Three independent experiments measured in triplicate were performed.

20S Proteasome ELISA

The levels of 20S proteasome in cells after treatment with different compounds were determined using a commercially available Proteasome ELISA kit according to the manufacturer's instruction (Enzo LifeSciences). Fluorescence was detected using a VictorX2 Multilabel Plate reader and data were normalized using DMSO-only treated cells as a control. Three independent experiments measured in triplicate were performed.

Proteasome Isolation

HTBH-Rpn11-HEK293T cells were treated with 5 μM of the indicated compounds for 16 hours after which cells were washed and collected by scraping in lysis buffer (100 mM NaCl, 50 mM sodium phosphate, 10% glycerol, 5 mM ATP, 1 mM DTT, 5 mM $MgCl_2$, 1× protease inhibitor (Roche), 1× phosphatase inhibitor (Roche), and 0.5% NP-40 (pH 7.5)). After a centrifugation step (21.100 g for 15 minutes) HTBH-tagged Rpn11-containing 26S proteasomes were isolated from the lysate by overnight incubation at 4°C with streptavidin beads. After 3 washes with wash buffer (50 mM Tris-HCl (pH 7.5)), 10% glycerol, 1 mM ATP), 26S proteasomes were cleaved from the beads by treatment with 1% TEV enzyme (protein expressed and purified in-house by the NKI protein facility) for 1 hour at 30°C in wash buffer. Protein concentration was determined using NanoDrop. For proteomic analysis, proteasome isolation was performed four separate times for each condition.

Real-Time PCR

Quantitative RT-PCR was performed to determine the mRNA expression levels of the proteasome subunits PSMB5 (β5), PSMB6 (β1), PSMB7 (β2) and the endogenous housekeeping gene β-glucuronidase (GUS) as a reference. Cells were treated with compounds as

previously described. mRNA was isolated using the Dynabeads mRNA DIRECT Purification kit (Thermo Fisher Scientific) according to the manufacturer's instructions after which cDNA was generated using SuperScript VILO cDNA Synthesis kit (Thermo Fisher Scientific). RT-PCR analysis was performed using SYBRgreen PCR Master Mix (Applied Biosciences) on a Chromo4 DNA Engine detection system (Bio-Rad) according to the manufacturer's instructions. Samples were amplified during 40 cycles of 15 seconds at 95°C and 60 seconds at 60°C. Relative mRNA expression levels of the target genes in each sample were calculated using the comparative cycle time (Ct) method (39) and normalized to either DMSO only-treated controls or non-targeting siRNA control. Primers and concentrations used for the quantitative real-time PCR were as follows:

PSMB5 forward (50 nM): 5'-CTTCAAGTTCCGCCATGGA-3'; PSMB5 reverse (300 nM): 5'-CCGTCTGGGAGGCAATGTAA-3'; PSMB6 forward (50 nM): 5'-AGGCATGACCAAGGA-AGAGTGT-3'; PSMB6 reverse (300 nM): 5'-GAGCCATCCCGCTCCAT-3'; PSMB7 forward (50 nM): 5'-TCGGTGTATGCTCCACCAGTT-3'; PSMB7 reverse (300 nM): 5'-GCAAAATCGGCTT-CCAAGAC-3'; GUS forward (300 nM): 5'-GAAAATATGTGGTTG GAGAGCTCATT-3'; GUS reverse (300 nM): 5'-CCGAGTGAAGATCCCCTTTTTA-3'; p38α MAPK forward (100 nM): 5'-AAGACTCGTTGGAACCCCAG-3'; p38α MAPK reverse (300 nM): 5'-TCCAGTAGGTCGAC-AGC CAG-3'; p38β MAPK forward (100 nM): 5'-AGCCCAGTGTCCCTCCTAA-3'; p38β MAPK reverse (300 nM): 5'-CCACAGGCAACCA CAAATCT-3'; p38γ MAPK forward (100 nM): 5'-AGCCCTCAGGCTGTGAATCT-3'; p38γ MAPK reverse (300 nM): 5'-CATATTTCTG GGCCT-TGGGT-3'; p38δ MAPK forward (100 nM): 5'-GCTCACCCCTTCTTTGAACC-3'; p38δ MAPK reverse (300 nM): 5'-TTCGTC CACGCTGAGTTTCT-3'.

Sample Preparation for SEC Proteomics Analysis

MelJuSo cells were lysed by brief sonication in the SEC-running buffer (150 mM NH_4Ac, pH 7.2) complemented with PhosStop and complete mini EDTA-free inhibitor cocktail (Roche). Lysates were clarified by centrifugation at 20-000*g* for 10 minutes at 4°C. Total protein concentration was determined with a Bradford assay and equal protein amounts of all treatment conditions were used for further sample preparation steps. The cell lysates were then concentrated through a Vivaspin 100 kDa molecular weight cutoff filter (Sartorius Stedim Biotech GmbH, Germany).

Concentrated samples were subsequently fractionated using an Åkta p900 LC system (Amersham Biosciences), equipped with a BioSep SEC s4000 column (600x7.8mm, 500Å, Phenomenex) with a flow of 450 μl/min. The Before the lysates a mix of molecular with warkers was run over the column (Gel Filtration Markers Kit for Protein Molecular Weigths 6,500-66,000 Da., Sigma-Aldrich). The eluted lysate sample was collected in fractions of 260 μl. 4M urea lysis buffer was added and fractions containing the proteasome were heated at 99°C for 5 minutes. Thereafter samples were reduced (4 mM DTT) and alkylated (8 mM iodoacetamide) and proteins were first digested using LysC (1: 75 enzyme/protein ratio, Wako) for 4 hours at 37°C and 2 times diluted with ammonium bicarbonate. Next, trypsin (1:50, Sigma-Aldrich) was added for further protein digestion, and the samples were incubated overnight at 37°C. The fully digested samples were acidified to 1% formic acid (Merck). Sample cleanup was performed using OASIS sample cleanup cartridges (Waters). Samples were then analyzed by LC-MS/MS.

Proteasome Enriched (Phospho)Proteomics Analysis

After proteasome affinity purification, samples were further diluted in 50 mM ammonium bicarbonate (pH 8.5) complemented with PhosStop and complete mini EDTA-free inhibitor cocktail (Roche) and digested as described above. Samples were desalted with Sep-Pak C18 cartridges (Waters), split in two replicates and dried down. One half of the samples was stored at -80°C before LC-MS/MS analysis and the other half of the sample was used for phosphorylated peptide enrichment. Phosphorylated peptides were enriched using Fe(III)-NTA cartridges (Agilent technologies) in an automated fashion using the AssayMAP BRAVO Platform (Agilent technologies). The cartridges were primed with 0.1% trifluoroacetic acid in acetonile and equilibrated with 80% acetonitrile/0.1% TFA (loading buffer). The samples were then dissolved in loading buffer and loaded onto the cartridges. The cartridges were washed with loading buffer and phosphorylated peptides were eluted with 1% ammonia directly into 10% FA, dried down and stored at -80°C untill LC-MS/MS analysis (Zhou et al., 2013).

Liquid Chromatography and Mass Spectrometry

All samples were reconstituted in 10% FA. In total. 40 % of the eluted phosphopeptides per sample were used for further analysis. All samples were analyzed using a Q-Exactive Plus Orbitrap instrument (Thermo Fisher Scientific, Bremen) connected to an Agilent 1290 HPLC system. The trap column was made of reversed phase C18 material (Dr. Maisch Reprosil, 3 μm,2 cm x 100 μm) and the analytical column was a 50 cm, 75 μm inner diameter capillary packed with Poroshell C18 material (Agilent, 120EC-C18, 2.7 μm). Both the trap column and analytical column were packed in-house. Solvent A consisted of 0.1% formic acid (Merck) in deionized water (Milli-Q, Millipore) and solvent B consisted of 0.1% formic acid in 80% acetonitrile (Biosolve). Peptides were first trapped at 50 μl/min with solvent A and then eluted with solvent B in a 120 min gradient at 100 nl/min: 0–10 min, 100 % solvent A; 10.1–105 min, 13–40 % solvent B; 105–108 min, 40-100 % solvent B; 108–109 min, 100 % solvent B; 109-110 min, 0–100 % solvent A; 110–120 min, 100 % solvent A. The Orbitrap was operated in a data-dependent manner, with the following settings: ESI voltage, 1700 V; Inlet Capillary Temperature 320°C; full-scan automatic gain control (AGC) target, 3×10^6 ions at 35 000 resolution; scan range, 350–1500 *m/z*; Orbitrap full-scan maximum injection time, 250 ms; MS2 scan AGC target, 5×10^4 ions at 17 500 resolution; maximum injection, 120 ms; normalized collision energy, 25; dynamic exclusion time, 30; isolation window 1.5 *m/z*; 10 MS2 scans per full scan.

Data Processing

RAW data files were processed with Max Quant (v1.5.2.8) and MS2 spectra were searched with the Andromeda search engine against the human proteome in UniProt (20.197 entries, downloaded on 16-07-18 from the uniprot.org website). Enzyme specificity was set to Trypsin/P and two missed cleavages were allowed. Both methionine oxidation and phospho (STY) were set as variable modifications and cysteine carbamidomethylation was set as fixed modification. Minimal peptide length was 7 amino acids. Mass tolerance was set to 20 ppm for peptide masses and 0,6 Da for fragmentation masses. FDR threshold was set to 1 % for identifications. Minimal ratio count was set to 2 for protein quantification and the functions ''LFQ'', ''match between runs'' and ''requantify'' were enabled. Perseus (v1.5.0.0) was used for data processing (Tyanova et al., 2016). A minimal localization probability of 0.75 was used for the phosphosite localization. To obtain multiple testing adjusted p-values, we performed Benjamini-Hochberg (Benjamini and Hochberg, 1995) in R v3.2.5.

QUANTIFICATION AND STATISTICAL ANALYSIS

Fluorescent signal of in-gel fluorescent scans was quantified using ImageQuant TL 8.1(GE Healthcare Life Sciences. Suc-LLVY-AMC conversion data are presented as mean ± SD of three independent experiments. The conversion rates in DMSO-treated control (CTR) cells and epoxomicin-treated cells (Epox) were set to 1 and 0, respectively. Intracellular fluorescence intensities determined by flow cytometry are presented as mean ± SD of three independent experiments. Cell viability experiments are presented as mean ± SD of three independent experiments. Statistical significance: ns = not significant, * = $P \leq 0.05$, ** = $P \leq 0.01$, *** = $P \leq 0.001$, and **** $P \leq 0.0001$ as determined by t-test.